ASTRO
A SPAR COMPANY

ASTRO AEROSPACE CORPORATION
6384 Via Real, Carpinteria, CA 93013-2993
Telephone (805) 684-6641
TWX 910-336-1144 FAX (805) 684-3372

STACBEAM II
FINAL REPORT, PHASE VI

by
Louis R. Adams
and
Angelika von Roos

AAC-TN-1134

23 April 1985

This report was prepared for the Jet Propulsion Laboratory, California Institute of Technology, sponsored by the National Aeronautics and Space Administration.

under Contract No. 955847

Prepared by

Astro Aerospace Corporation
6384 Via Real
Carpinteria, CA 93013

TABLE OF CONTENTS

SECTION 1: INTRODUCTION 1-1

SECTION 2: STACBEAM MODIFICATION 2-1

2.1 Tubular Members 2-1
2.2 Joint Designs 2-2
2.2.1 Joint Body 2-2
2.3 Midhinges 2-4
2.3.1 Nearly-Over-Center Hinge 2-4
2.4 Dynamic Analysis 2-5

SECTION 3: BEAM FABRICATION 3-1

3.1 Procurement 3-1
3.2 Machining 3-1
3.3 Assembly of Hinge Parts 3-2
3.3.1 Corner Body Assembly 3-2
3.3.2 Longeron Midhinge Assembly 3-2
3.3.3 Diagonal Midhinge Assembly 3-2
3.4 Beam Assembly 3-2

SECTION 4: STACBEAM/SOLAR ARRAY SYSTEM PERFORMANCE 4-1

4.1 System Mass 4-1
4.2 Beam Stiffness 4-2
4.2.1 Longeron Stiffness 4-3
4.2.2 Diagonal Stiffness 4-5
4.3 System Frequency 4-10
4.4 Status and Potential 4-11

SECTION 5: RETRACTION AND CONTINUOUS DEPLOYMENT CONCEPTS 5-1

5.1 Continuous Deployment 5-2
5.1.1 Lead Screw Design 5-2
5.2 Retraction 5-9
5.3 Solar Blanket Deployment 5-10

SECTION 6: CONCLUSIONS AND RECOMMENDATIONS 6-1

APPENDIX A: NEARLY-OVER-CENTER HINGE ANALYSIS A-1

APPENDIX B: BEAM DEFLECTION ANALYSIS B-1

LIST OF TABLES AND FIGURES

Table 1-1. Solar Array System Design Goals 1-4

Figure 2-1. Joint body 2-3
Figure 2-2. STACBEAM solar array dynamic model 2-6
Figure 2-3. Vibration modes of STACBEAM solar blanket system 2-7

Figure 3-1. Corner body assembly 3-3
Figure 3-2. Longeron midhinge assembly 3-4
Figure 3-3. Diagonal midhinge assembly 3-5
Figure 3-4. Sixteen-bay STACBEAM I-II 3-6

Figure 4-1. Individual longeron stiffness test 4-4
Figure 4-2. Longeron extension test 4-6
Figure 4-3. Individual diagonal stiffness test 4-8
Figure 4-4. Beam lateral stiffness test 4-9
Figure 4-5 System Performance 4-10

Figure 5-1. Deployer, launch configuration 5-3
Figure 5-2. Deployer, extended 5-4
Figure 5-3. Deployer in operation 5-5
Figure 5-4. Deployer detail with deploying bay 5-6
Figure 5-5. Deployer detail with lifting stack and bay 5-7
Figure 5-6. Deployer detail with lifting bay and stationary stack 5-8

ABSTRACT

The STACBEAM (Stacking Triangular Articulated Compact Beam), which had been conceived in an early part of this contract and built as an engineering model for proof-of-concept, was redesigned and built for structural evaluation. The proof-of-concept beam, STACBEAM I, and the structural evaluation model, STACBEAM II, differ primarily in that the former had graphite/epoxy rod members and the latter has tubular members which result in a four-fold increase in beam strength. Changes were also made to reduce compliance, notably in hinge pin design and in nearly-over-center hinges.

A finite-element analysis was conducted to determine resonant frequencies of the cantilevered system of STACBEAM and the solar array. The results confirm the overall design for a 0.2-Hz cantilever frequency and a blanket frequency near 0.6 Hz.

Tests (both of individual members and on the whole beam) were conducted on STACBEAM II to determine its stiffness properties. These tests and accompanying analysis show that the solar array system, supported by STACBEAM II in its present status, exceeds the recently flown Solar Array Flight Experiment (SAFE) array frequency by more than a factor of 2. The mass of the STACBEAM II system is nearly 40 kg less than the SAFE system.

Conceptual investigations of beam retraction and continuous deployment were also conducted.

SECTION 1
INTRODUCTION

An investigation is being conducted by Astro Aerospace Corporation (Astro) for Jet Propulsion Laboratory in which efficient structures for geosynchronous spacecraft solar arrays are being developed. Recent developments in solar blanket technology, including the introduction of ultrathin (50-micrometer) silicon solar cells with conversion efficiencies approaching 15 percent, have resulted in a significant increase in blanket specific power (Ref. 1). System specific power depends not only on blanket mass but also on the masses of the support structure and deployment mechanism. These masses must clearly be reduced, not only to minimize launch weight, but also to increase array natural frequency.

The solar array system natural frequency should be kept high in order to reduce the demands on the attitude control system. This goal is approached by decreasing system mass, by increasing structural stiffness, and by partitioning the blanket. The previous phases of the contract area were reported in References 2, 3, and 4 and are described as follows:

Phase I, Concept Generation: Packaging and deploying concepts for geosynchronous solar arrays were investigated.

Phase II, Parametric Analysis: Three candidate structures were evaluated in terms of stiffness, mass, and package size.

Phase III: Point Design Evaluation: The STACBEAM (Stacking Triangular Articulated Compact Beam) was specified.

Phase IV: STACBEAM Development: A full-scale (0.9-m diameter, 0.428-m baylength, and 3.2-mm member size) beam was built.

Phase V: STACBEAM Deployer Development: An engineering model of an electrically automated deployer was built.

As a result of this work, a highly efficient structure for deploying a solar array has been developed. Advantages of the STACBEAM as the structural support of a solar array, as compared to the recently flown Solar Array Flight Experiment (SAFE) system are:

- o The STACBEAM does not rotate during deployment (as SAFE did), thus allowing periodic attachment of the blanket to the beam. This greatly increases blanket stiffness so that system frequency is increased.
- o STACBEAM members rotate about single-degree-of-freedom hinges which are oriented so that the packaged and deployed conditions are unstrained. This approach allows the use of graphite/epoxy (Gr/Ep) composites which have relatively low strain capability but have extremely high specific stiffness (modulus/density).

These STACBEAM advantages result in lower system mass and higher system natural frequency.

STACBEAM I was built in Phase IV. It served as a proof-of-concept in terms of hinge positions and orientations, packaging ratio, mass, and beam strength. In Phase V of this contract, a reciprocating-type deployer was constructed which deployed STACBEAM I by lifting each bay to full extension, releasing it, and lowering to grasp the next bay in succession.

Phase VI was directed toward improving STACBEAM I as a structure and is summarized as follows:

- o The beam design was changed to create STACBEAM II. Design changes included:
  - Hinge pin modification for better retention
  - Hinge modification to reduce compliance and increase alignment preload
  - Hinge modification to allow for the use of Gr/Ep tubular members instead of rods
- o The use of standoffs for blanket attachment was investigated. This included a study of the kinematics of beam and blanket deployment and a finite-element analysis of system frequency.
- o An eight-bay model of STACBEAM II was constructed incorporating the design modifications described above. Tests were conducted on the beam and on individual members in order to determine beam stiffness and how it is affected by member compliance. Using these test results, it was found that the performance of a system consisting of a 31-m STACBEAM, a solar array attached at 3.5-m intervals, a deployer, and other required components is better than the SAFE array both in terms of mass and frequency.

No provision was made previously for retraction of the beam during Phase VI. A new method of deployment was also investigated which is continuous in operation and has retraction capability. The main component of this new deployer is a set of three lead screws which interface directly with

the three corners of the batten frames. Synchronized rotation of the lead screws causes the beam to deploy or retract, depending on the direction of the lead screw rotation. Additional mechanisms hold the base of the deploying or retracting bay and initiate folding of members during retraction.

System requirements, including those of the beam, are listed in Table 1-1.

TABLE 1-1. SOLAR ARRAY SYSTEM DESIGN GOALS.

SYSTEM	
Array power	23.9 kW
Blanket mass	53 kg
Blanket area	126 m^2 (4 by 31.5 m)
System mass	88 kg
System frequency	0.2 Hz
Blanket frequency	0.6 Hz
STACBEAM	
Diameter	0.9 m
Bay length	0.43 m
Mass	10 kg
Member stiffness, EA	830,000 N
Packaging ratio	42.25 to 1
Blanket attachment interval	8 bays

SECTION 2
STACBEAM MODIFICATION

A previous phase of this contract (IV) consisted entirely of the design and fabrication of an engineering model of the STACBEAM. Its members are all graphite/epoxy (Gr/Ep) rods of 3.18-mm diameter (0.125-in.), and the hinges are machined aluminum. Hinge pins are 1-mm-diameter (0.040-in.) steel rods. The longerons and diagonals, which fold for packaging, have spring-loaded midhinges to provide alignment preloads when deployed. That beam, which has been termed STACBEAM I, verified the following:

- o Hinge positions and orientations are correct for strain-free deployed and packaged configurations
- o Predicted mass per unit length is achievable
- o Beam ultimate bending moment is achievable

STACBEAM I was designed and constructed in order to serve as a proof-of-concept demonstration model. Observation and test of this beam indicated the need for the following improvements:

- o Gr/Ep rods, which were used because of availability, should be replaced by tubes of the same area but of larger diameter for increased beam strength.
- o Hinge pins should be modified for positive retention and to reduce hinge compliance.
- o Nearly-over-center hinges in folding members should be modified to produce greater alignment force.

STACBEAM II, developed during this phase of the contract, incorporates these improvements and is compared to STACBEAM I as follows.

2.1 TUBULAR MEMBERS

The difference between members of STACBEAM I and II are illustrated in the following table:

	STACBEAM I	STACBEAM II
OD, mm (in.)	3.18 (0.125)	5.08 (0.200)
ID, mm (in.)		3.96 (0.156)
Area, mm^2 (in^2)	7.94 (0.0123)	7.95 (0.0123)
Area moment of inertia, mm^4 (in^4)	5.01 (1.21×10^{-5})	20.62 (4.95×10^{-5})

Since members of both beams are composed of Gr/Ep, the modulus E and density ρ are approximately the same for tubular or rod members. Therefore, because the areas are equal, STACBEAM II members have the same linear density ρA and stiffness EA as in STACBEAM I, and beam mass and stiffness are unchanged. Beam strength is increased by a factor of 4.1, however, due to increased Euler buckling capacity of the longeron tubes which increases the ultimate beam bending moment.

2.2 JOINT DESIGNS

The design of the joints was modified to accommodate the change from rods to tubular members and the use of larger hinge pins. The positions and orientations of hinge pins and deployer interface flanges remain the same as STACBEAM I.

2.2.1 Joint Body

The joint body is shown in sketch form in Figure 2-1. It serves four functions:

- o Longeron end hinge
- o Diagonal end hinge
- o Batten corner fitting
- o Deployer interface

2.2.1.1 LONGERON END HINGES

The hinges at the ends of the longerons are all identical. They are larger than those of STACBEAM I, having larger and longer holes. Each end is pinned to a joint body by a shaft which is threaded on one end for retention. The hinge pin passes through the member centerline and is placed so the packaged longerons stack on top of each other and are aligned with the beam radius.

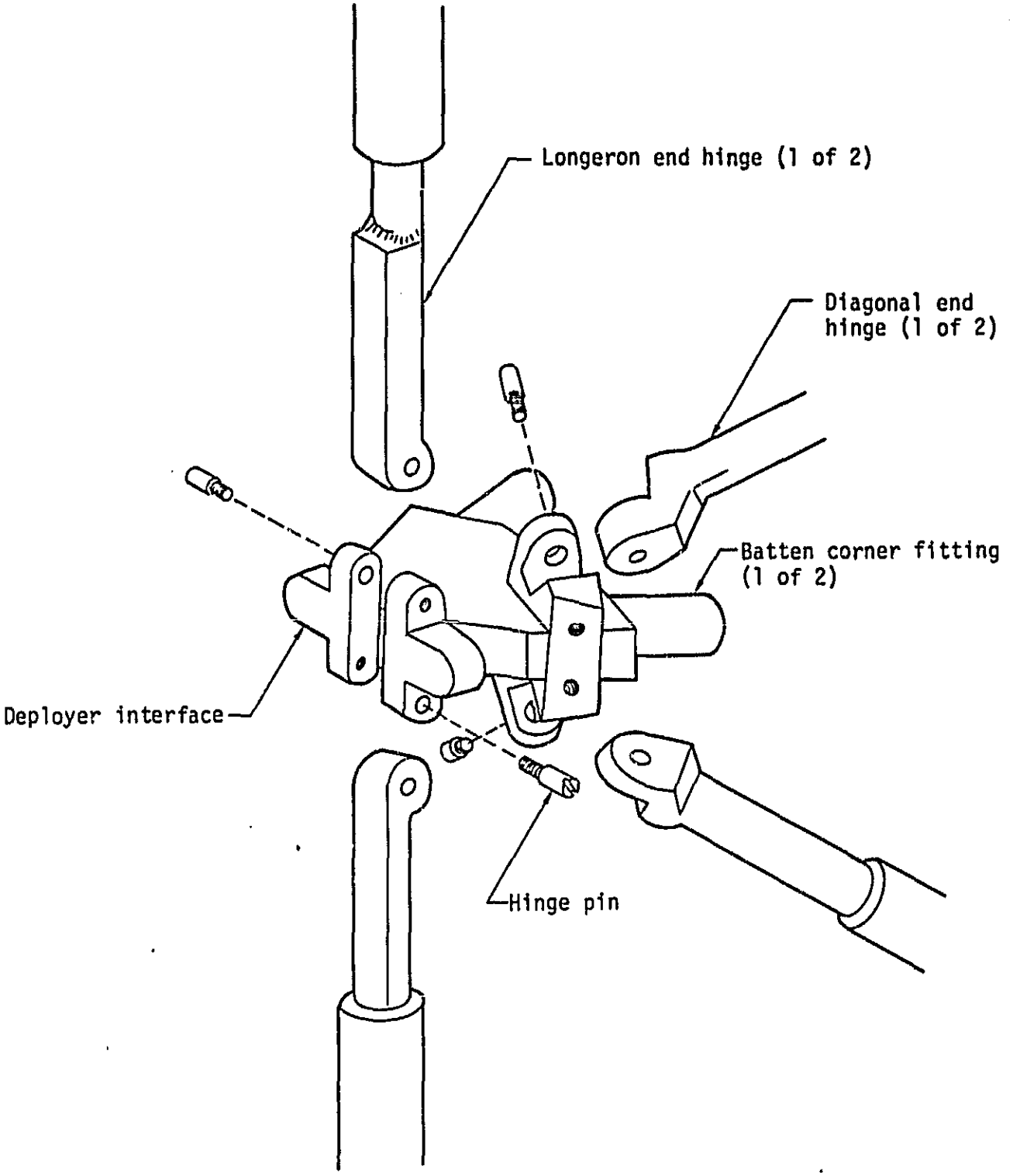

Figure 2-1. Joint body. 203A

2.2.1.2 DIAGONAL END HINGES

The hinges at the ends of the diagonals are oriented as in STACBEAM I and are pinned with threaded shafts, similar to those in the longeron end hinges.

2.2.1.3 BATTEN FITTING

The battens are not hinged but are bonded rigidly at each end to the joint bodies.

2.2.1.4 DEPLOYER INTERFACE

The deployer for STACBEAM II is the same as that for STACBEAM I. Interface to the deployer is made through three features on the joint body:

1. Protrusions, one on each side, extend into guides on the deployer
2. The protrusions also mate with starwheels which temporarily hold the beam
3. The posts on which the longerons hinge interface to an articulating lifting device.

NOTE: These features are illustrated in Figures 4 and 5 of Reference 4.

2.3 MIDHINGES

Hinges are required at the midspans of the longerons and diagonals which fold during packaging. These hinges must provide positive "locking" forces in the deployed configuration in order that the Euler buckling capability of each member can be realized.

2.3.1 Nearly-Over-Center Hinge

The midhinges of STACBEAM I were early attempts in the design of preloaded hinges. The concepts tried included a ball-and-detent mechanism for the diagonals which was abandoned in favor of a spring-link assembly. The longeron midhinges were of the nearly-over-center type. Problems were observed in the function of these hinges, some of which were noted in the Phase IV report for this contract. The margin of preload on the longerons and diagonals was too small, resulting in unintentional longeron folding due to bumping of a member. This also reduced the shear strength of the beam because of the lower diagonal buckling capacity.

It was necessary to increase the moment-generating capability of the midhinges to obtain a better hinge with more deployment force. Appendix A shows how moments generated by springs in the nearly-over-center assembly relate to the bending moment required to open the hinge. The results of this analysis show that:

- Of the four possible spring positions (at the four pin locations), only one is efficient in terms of generating high bending moment. Two of the positions are inefficient due to spring unwinding during deployment; one simply does not produce moment multiplication. Position c described in Appendix A is preferred because it produces high moment multiplication and does not unwind during deployment.
- The angle between the links must be very small in the fully deployed position.
- The unsprung link must be properly oriented so that its compressive load not only preloads the joint but also produces the desired moment between the hinged members.

2.4 DYNAMIC ANALYSIS

The design case on which this STACBEAM and solar array system was based used a simplified model for determining its natural frequency. It was assumed as a first approximation that the lowest vibration mode was close to that of a simple cantilever at 0.2 Hz and a closed solution was obtained. Since it is possible that other modes (transverse blanket vibration, torsion, etc.) may be of lower frequency than this, a finite-element computer analysis was performed to determine the ten lowest modes of vibration. The finite-element model is shown in Figure 2-2. The beam and blanket are both 31.5 meters long, and attachments are made at 3.5-meter intervals.

The longerons, battens, diagonals, and standoffs have identical properties: $E = 1.1 \times 10^{11}$ N/m^2, $A = 7.94 \times 10^{-6}$ m^2, $\rho = 1520$ kg/m^3, $k = 1.75$. The blanket mass is 54 kg, distributed over 126 m^2. The blanket is stiffened by lateral members of stiffness $EI = 31$ Nm^2, and is under tension of 24 N.

The results of these analyses are shown in Figure 2-3. As originally assumed, the lowest frequency mode is the primary cantilever mode, at 0.17 Hz, in a direction perpendicular to the blanket. The next higher frequency, at 0.21 Hz, is the alternate primary mode vibrating parallel to the blanket. The

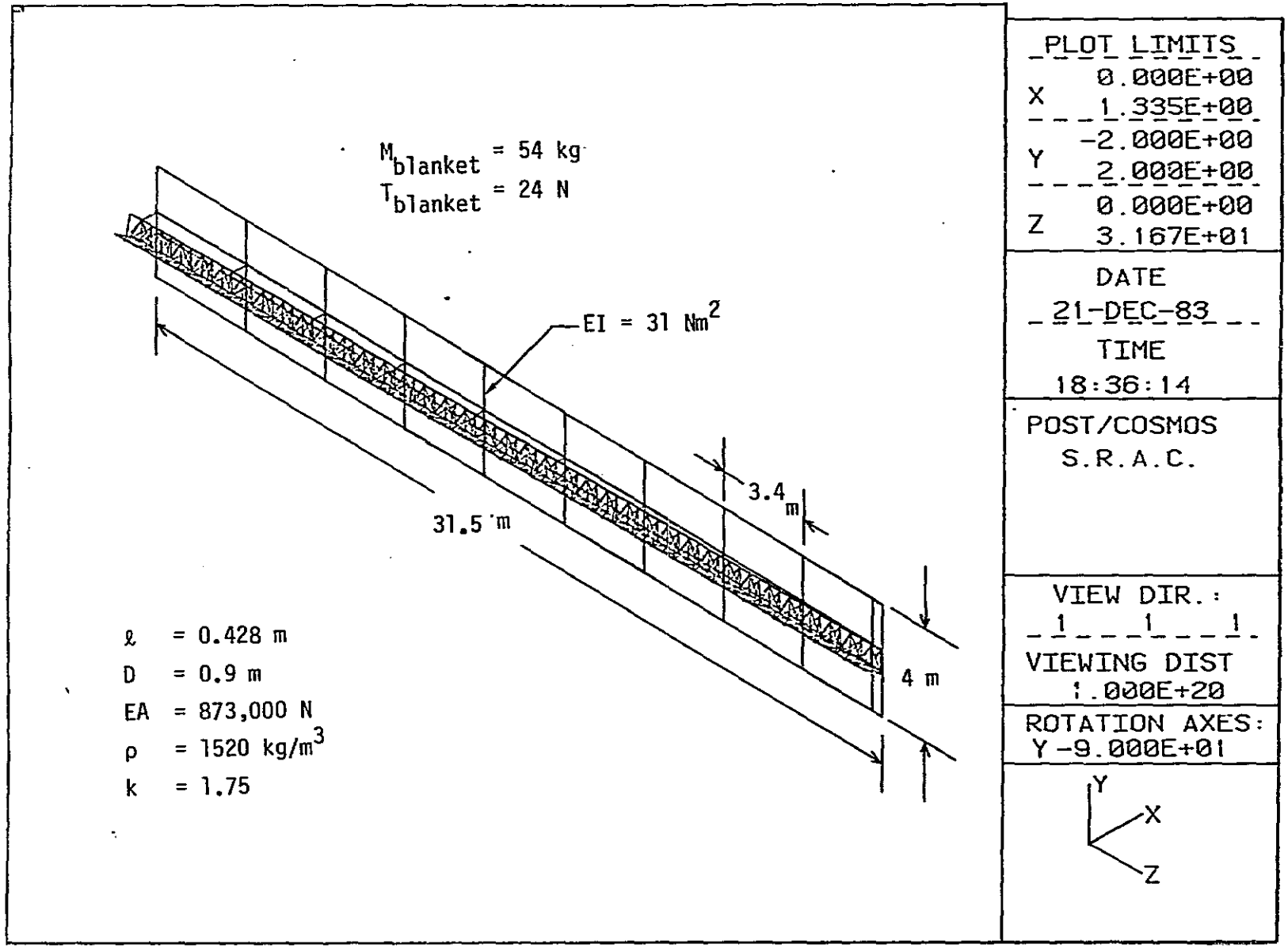

Figure 2-2. STACBEAM solar array dynamic model.

199A

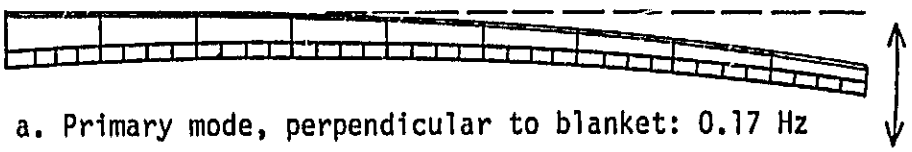

a. Primary mode, perpendicular to blanket: 0.17 Hz

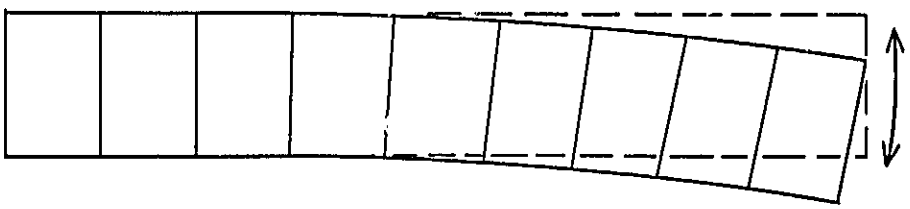

b. Primary mode, parallel to blanket: 0.21 Hz

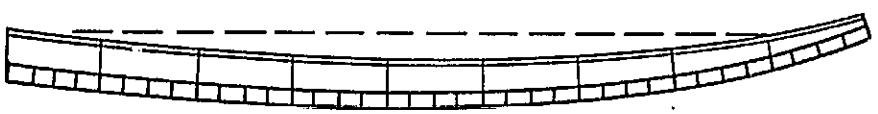

c. Secondary mode: 0.56 Hz

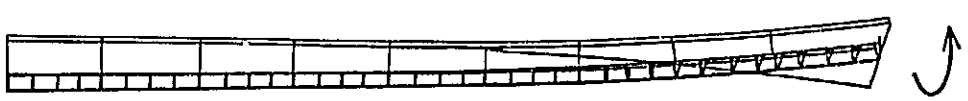

d. Torsion: 0.59 Hz

e. Mixed modes: ~0.60 Hz

Figure 2-3. Vibration modes of STACBEAM solar blanket system. 201A

next eight frequency modes are all clustered about f = 0.6 Hz. With the exception of the fifth mode, which is torsion at 0.59 Hz, all are higher harmonics of beam and/or blanket vibration.

These results substantiate quite well the initial point design which assumed that the blanket fundamental frequency is three times that of the beam and blanket together. The blanket stiffening battens, as well as the tension level in the blanket, were designed so that this blanket frequency factor is realized.

SECTION 3
BEAM FABRICATION

Fabrication of the beam involved several tasks: material procurement and test, hinge machining, assembly of hinge parts, fixturing, bonding, and beam assembly. The fabrication of this beam was similar to that of STACBEAM I. For a detailed view of fixturing and bonding procedures, see Reference 3.

3.1 PROCUREMENT

The specification for the graphite/epoxy composite tubing required a finished tube modulus of $E > 1.03 \times 10^{11}$ N/m^2 (15×10^6 psi) and a maximum deviation from a straight line of 1/1000 of its length (L/1000) over a length of 0.75 m (30 in.). Tube outside diameter was specified as 5.08 mm (0.200 in.) and wall thickness 0.56 mm (0.22 in.). Fiber orientation was to be parallel to the tube axis.

These requirements were met by tubing supplied by Dittmer and Dacy of San Diego. The elastic modulus was measured statically by a three-point bending test and by determining the Euler buckling load, and dynamically by determining the free-free frequency (that is, the natural frequency of the unrestrained beam). These tests yielded moduli of 1.6, 1.2, and 1.2×10^{11} N/m^2, respectively, all of which exceeded the specification.

Straightness was determined by comparison to flat surfaces. Of the 150 pieces received, each of 0.88-m (34 in.) length, 50 percent exceeded the L/1000 straightness criterion and 20 percent were better than L/5000.

3.2 MACHINING

Fabrication of the hinge parts was done by a vendor outside of the company using basic machine shop practices. The material used in the hinges was the same as that used on STACBEAM I, i.e., aluminum alloy 2024-T351, which was chosen for its low cost and availability.

3.3 ASSEMBLY OF HINGE PARTS

There were three groups of parts: those for assembly of the corner bodies, those for longeron midhinges, and those for diagonal midhinges. The hinges were assembled freehand using pins which are threaded on one end.

3.3.1 Corner Body Assembly

Figure 3-1 shows an exploded view of the parts which make up the corner body. Some parts are assembled using EA 934 adhesive so that a rigid body is achieved. Two longeron end fittings and two diagonal end fittings hinge to the corner body.

3.3.2 Longeron Midhinge Assembly

The parts which make up this assembly are shown in Figure 3-2. The spring which bears on the upper link is of 1.016-mm-diameter (0.040 in.) spring steel with one turn. Spring placement is at Point c, shown in Figure A-1 in Appendix A, for the greatest moment multiplication. This hinge rotates through 180 degrees from packaged to deployed configuration and packages so that its height is equal to two longeron diameters.

3.3.3 Diagonal Midhinge Assembly

The parts which make up this assembly are shown in Figure 3-3. The spring for this hinge is the same as that used in the longeron midhinge. The longeron midhinge had to be modified for use in the diagonal, however, because when the beam is packaged there is not enough space in the center of the package for the links of a longeron-type midhinge. Since the diagonal midhinge rotates only between 120 and 180 degrees for its packaged and deployed configurations, respectively, there was enough space for the links to be placed inside of the bend, away from the center of the package (compare Figures 3-2 and 3-3).

3.4 BEAM ASSEMBLY

Eight bays of STACBEAM II were assembled and mounted for test as described in the next section. These eight bays were then attached to the eight-bay STACBEAM I engineering model by bonding the rod members of I into the tubular members of II. This 16-bay beam is shown in Figure 3-4.

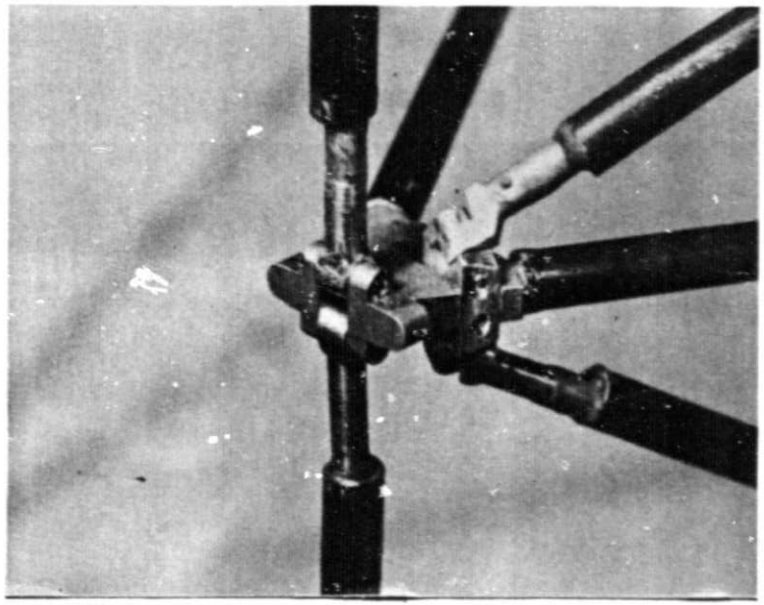

Deployed P090

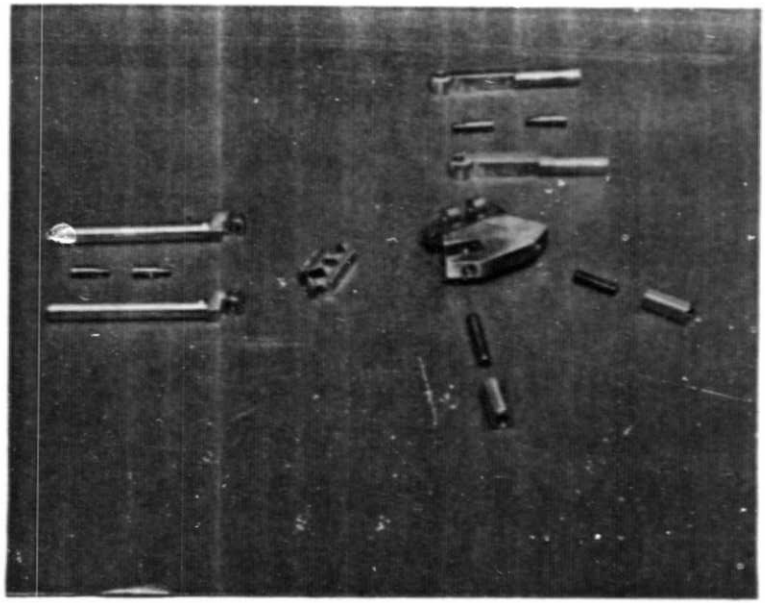

Exploded view P091

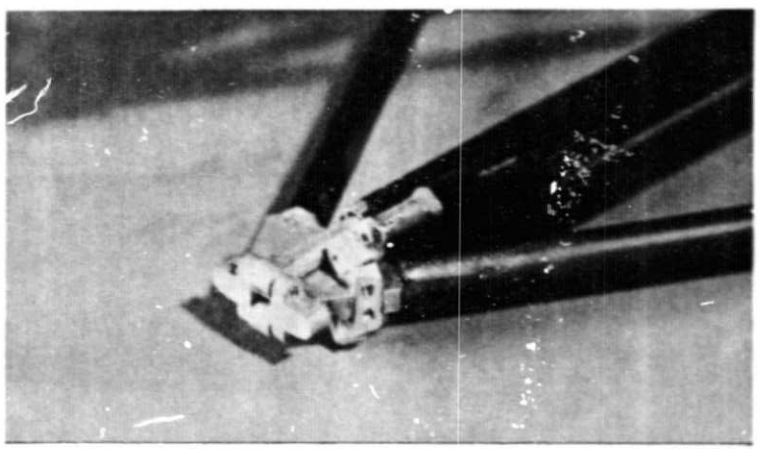

Packaged P092

Figure 3-1. Corner body assembly.

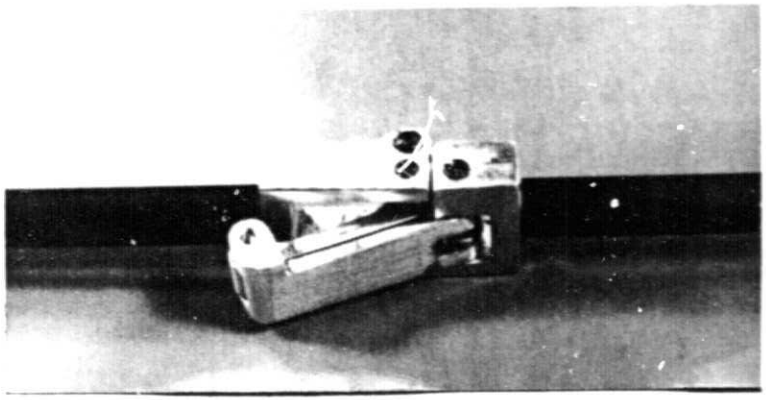

Deployed P093

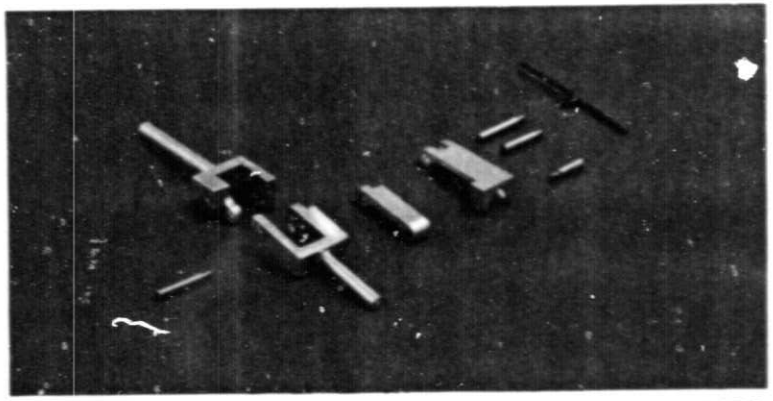

Exploded view P094

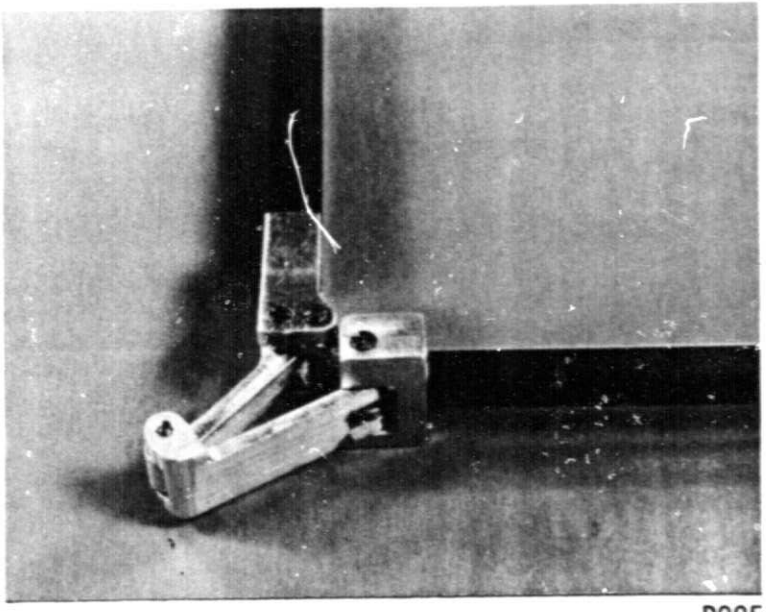

Partially deployed P095

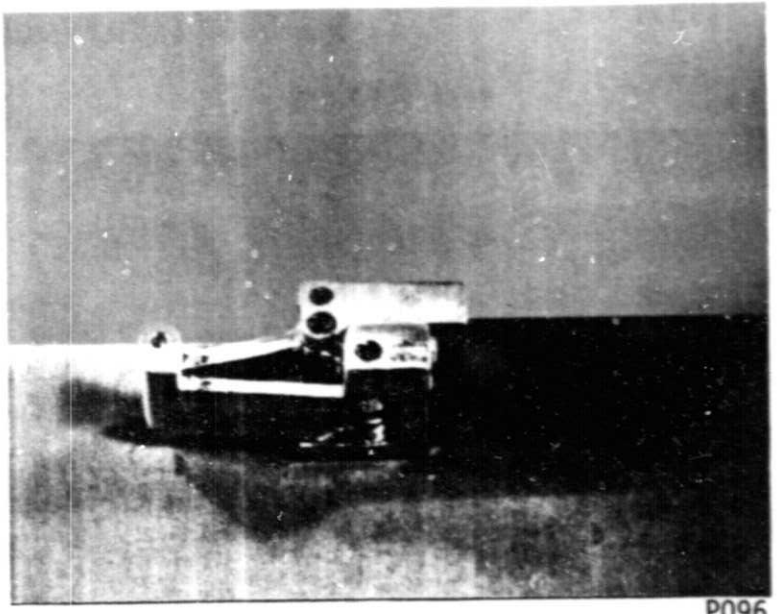

Packaged P096

Figure 3-2. Longeron midhinge assembly.

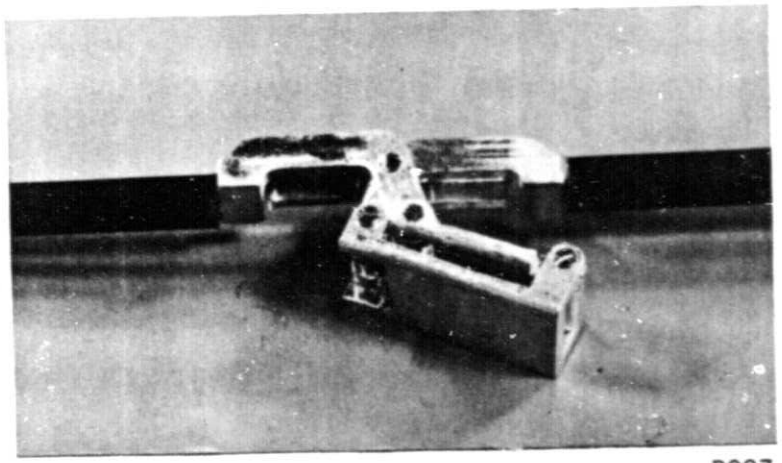

Deployed P097

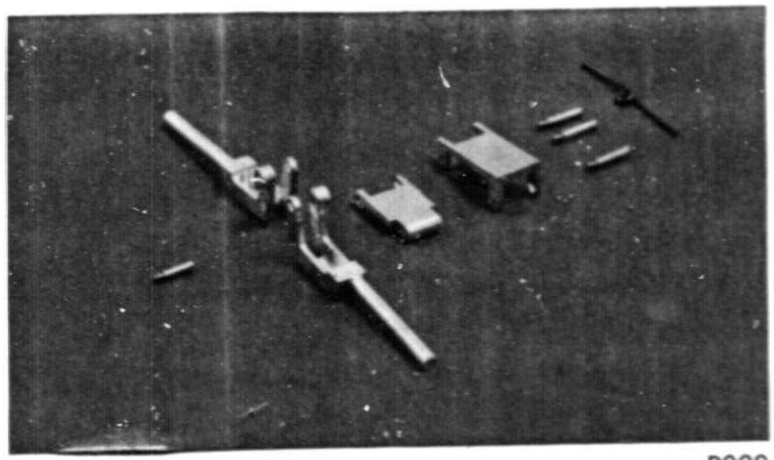

Exploded view P098

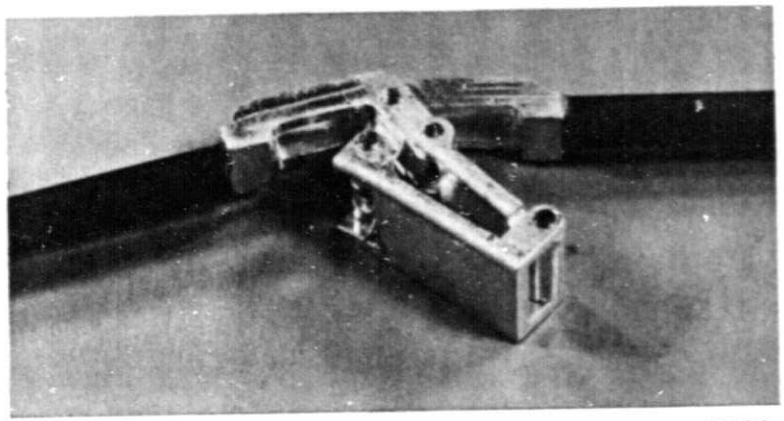

Partially deployed P099

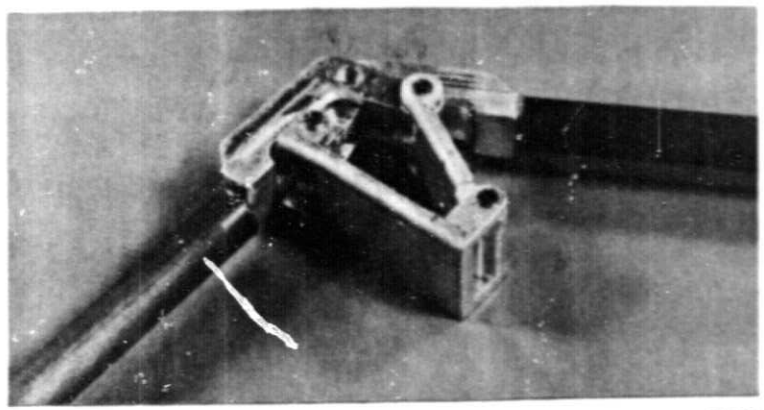

Packaged P100

Figure 3-3. Diagonal midhinge assembly.

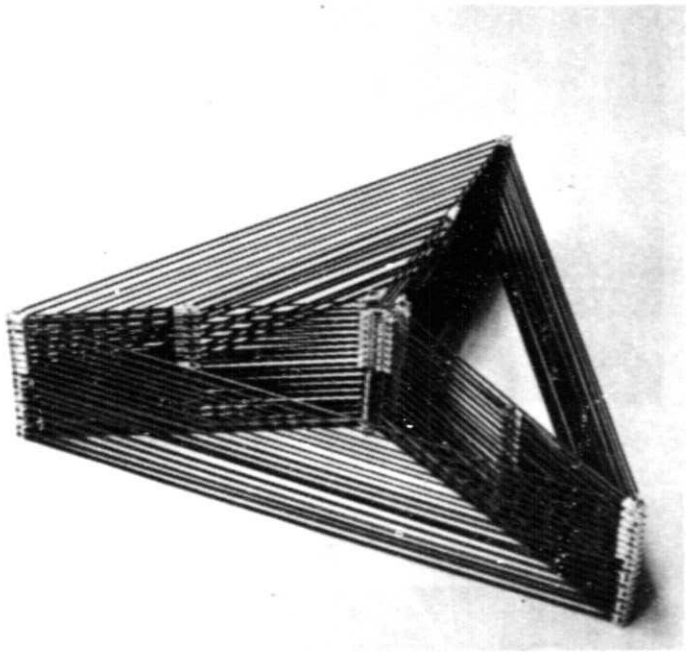

a. Packaged 85-P012

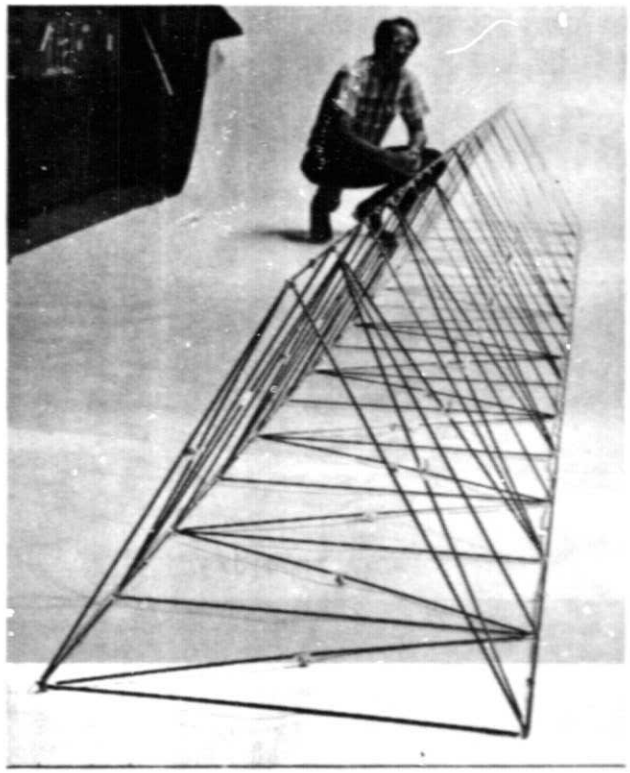

b. Deployed 85-P013

Figure 3-4. Sixteen-bay STACBEAM I-II.

SECTION 4
STACBEAM/SOLAR ARRAY SYSTEM PERFORMANCE

The design specification for the STACBEAM in the solar array system was based on achievement of high cantilever frequency and low total mass. A goal was postulated in which the frequency was 0.20 Hz and the total mass was 88 kg. In this section, the status of the design effort will be assessed in these terms.

Because the STACBEAM is a hinged beam, it is expected that hinge compliance will have an effect toward lessening beam stiffness. The 0.20-Hz frequency goal was based on ideal member stiffness; that is, no stiffness knockdown was assumed due to longeron hinge compliance. Therefore, the primary intent of this section is to determine the extent of system frequency (and performance) reduction due to hinge compliance.

4.1 SYSTEM MASS

The mass of the system, as outlined in Table III of Reference 2, includes the masses of the beam and deployer, solar blanket, and all associated hardware. The early estimates were based on mathematical models which considered dynamic requirements and material properties in predicting beam and deployer masses. These can be updated since engineering models have been built. The eight-bay models of STACBEAMs I and II weighed 0.862 and 1.032 kg, respectively, and adjustments for titanium replacement of the aluminum hinges yield a probable linear beam mass of 0.39 kg/m. The full-length (31.5-m) beam mass then is 12.1 kg.

The deployer of Phase V, which was of flight dimensions and operation but contained no composite materials to obtain stiffness, weighed 15.5 kg. The complete system with the component masses in place of the original estimates has a mass of 101 kg. This system mass is the ordinate of a data point defining the experimental status of the STACBEAM/solar array system (See Figure 4-5). The abscissa is the system cantilever frequency which is determined as follows.

4.2 BEAM STIFFNESS

The cantilever frequency of the system including the STACBEAM and solar array depends on the vibrating mass and the stiffness of the beam. Beam bending stiffness depends primarily on longeron compliance, but diagonal compliance also enters in. Appendix B examines the relation between load and deflection in a beam of known longeron and diagonal compliance. It is shown there that beam deflection X_d is related to diagonal stiffness EA_d as

$$X_d = \frac{16}{9} \frac{F}{EA_d} L \tag{4-1}$$

where F is the load exerted laterally on the beam at distance L from the fixed root.

It is also shown that the deflection X_ℓ is related to longeron stiffness EA_ℓ as

$$X_\ell = \frac{8}{9} \frac{F}{EA_\ell} \frac{L^3}{D^2} \tag{4-2}$$

where D is the beam diameter. These expressions can be combined to give the total beam deflection

$$X = X_\ell + X_d$$

$$X = \frac{8}{9} \frac{F}{EA_\ell} \frac{L^3}{D^2} (1 + k_s) \tag{4-3}$$

where

$$k_s = 2 \frac{EA_\ell}{EA_d} \frac{D^2}{L^2}$$

is the diagonal shear penalty. Thus a knowledge of individual member stiffnesses yields a prediction of beam stiffness.

The stiffness EA of the Gr/Ep tubing is, from test,

$$(1.2 \times 10^{11}\ N/m^2)\ (7.94 \times 10^{-6}\ m^2) = 960{,}000\ N$$

Placement of hinges along the load path reduces the member stiffness from this reference value. The product EA is then treated as a single term and reflects a measured value.

4.2.1 Longeron Stiffness

Two sets of tests were conducted to determine longeron stiffness EA_{ℓ}. Tests were conducted on individual longerons to determine the effect of the midhinge, and an eight-bay beam was tested axially to determine overall longeron stiffness.

4.2.1.1 MIDHINGE EFFECT

Figure 4-1 shows the setup for measuring the stiffness of individual longerons. Axial loads varying from 90-N (20-pound) compression to 90-N tension were applied, depending on the arrangement in which the weights were attached. The test setup measured deflections due to compliances of the midhinge and the 0.32-m length of the Gr/Ep tube.

Results from these tests are shown in Figure 4-1. The force-deflection curves do not change slope significantly on either side of the unloaded point which indicates that longeron stiffness is the same in tension or compression with a value near 1.07×10^6 N/m. The longeron midhinge, as it is constructed with aluminum alloy and nominally close-fitting hinge pins, decreases the member stiffness to about half of the reference value. The compliance of the midhinge may be determined by considering that the total member compliance is the sum of the hinge and tube compliances

$$\delta = FC_{\ell m} + \frac{F}{EA}\,\ell$$

where δ is the deflection at load F. Then

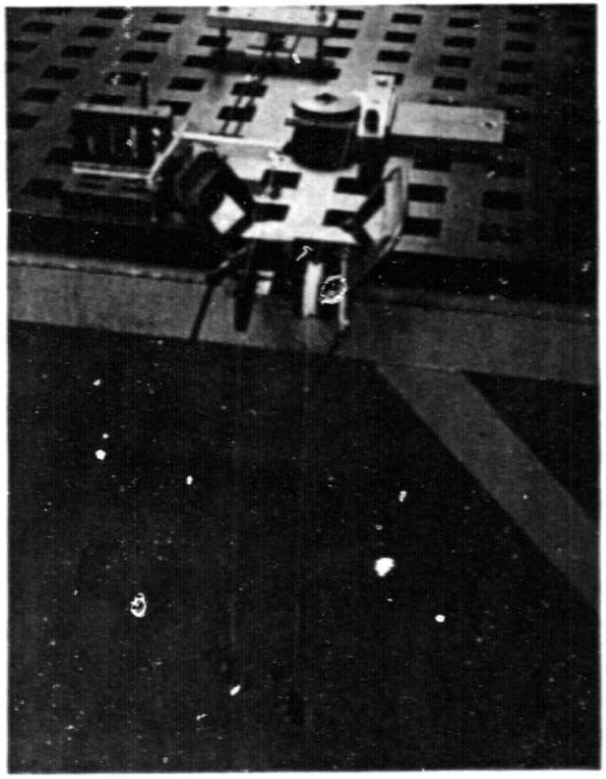

P101

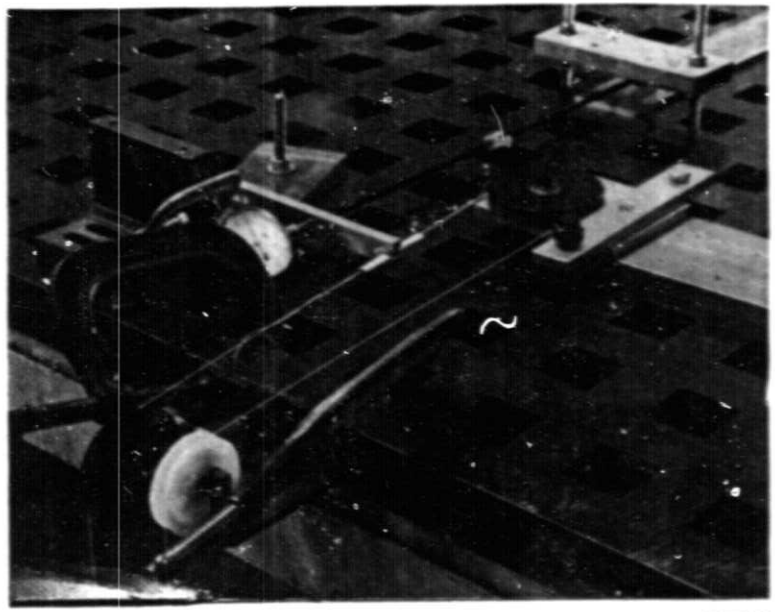

P102

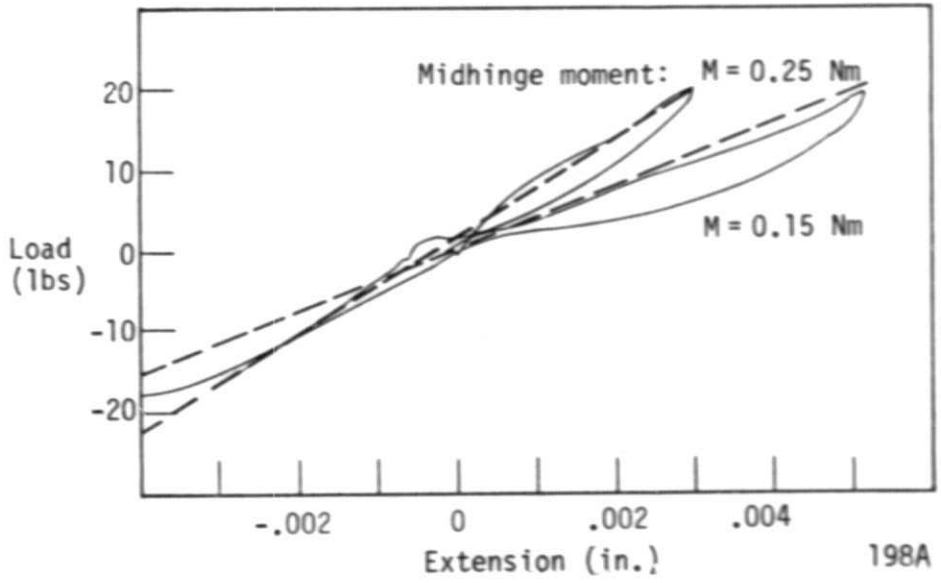

Figure 4-1. Individual longeron stiffness test.

$$C_{\ell m} = \frac{\delta}{F} - \frac{\ell}{EA}$$

$$= \frac{1}{1.07 \times 10^6 \text{ N/m}} - \frac{0.32 \text{ m}}{960{,}000 \text{ N}}$$

$$= 6.0 \times 10^{-7} \text{ m/N}$$

is the compliance of the longeron midhinge. The moment-generating capability of the midhinge appears to have a direct effect on the longeron stiffness: the greater the moment, the greater the stiffness.

4.2.1.2 TOTAL LONGERON

An eight-bay STACBEAM II test article was cantilevered horizontally, and an axial load was applied at the tip at one of the lower longeron positions as shown in Figure 4-2. The eight longerons which connect this point to the root of the beam are initially in compression due to gravity, with those near the root being more highly loaded. This loaded the root longerons to 12.8 N (2.85 pounds) to balance the cantilever moment. The test loads were directed away from the beam so that the longeron compressive preload was relieved.

The resulting load-deflection curve, also shown in Figure 4-2, shows no deadband. This is expected because the eight connected longerons are in different loading states so that only one longeron is unloaded at a time. The longeron axial stiffness obtained from this experiment was

$$EA_\ell = 300{,}000 \text{ N}$$

The longeron compliance due to each of the two end hinges was

$$C_{\ell_e} = 2.5 \times 10^{-7} \text{ m/N}$$

4.2.2 Diagonal Stiffness

In a short beam where the length of the beam is not much greater than the beam diameter, shear plays a large part. Therefore, the stiffness of the

$$C_{\ell m} = \frac{\delta}{F} - \frac{\ell}{EA}$$

$$= \frac{1}{1.07 \times 10^{6} \text{ N/m}} - \frac{0.32 \text{ m}}{960{,}000 \text{ N}}$$

$$= 6.0 \times 10^{-7} \text{ m/N}$$

is the compliance of the longeron midhinge. The moment-generating capability of the midhinge appears to have a direct effect on the longeron stiffness: the greater the moment, the greater the stiffness.

4.2.1.2 TOTAL LONGERON

An eight-bay STACBEAM II test article was cantilevered horizontally, and an axial load was applied at the tip at one of the lower longeron positions as shown in Figure 4-2. The eight longerons which connect this point to the root of the beam are initially in compression due to gravity, with those near the root being more highly loaded. This loaded the root longerons to 12.8 N (2.85 pounds) to balance the cantilever moment. The test loads were directed away from the beam so that the longeron compressive preload was relieved.

The resulting load-deflection curve, also shown in Figure 4-2, shows no deadband. This is expected because the eight connected longerons are in different loading states so that only one longeron is unloaded at a time. The longeron axial stiffness obtained from this experiment was

$$EA_{\ell} = 300{,}000 \text{ N}$$

The longeron compliance due to each of the two end hinges was

$$C_{\ell_e} = 2.5 \times 10^{-7} \text{ m/N}$$

4.2.2 Diagonal Stiffness

In a short beam where the length of the beam is not much greater than the beam diameter, shear plays a large part. Therefore, the stiffness of the

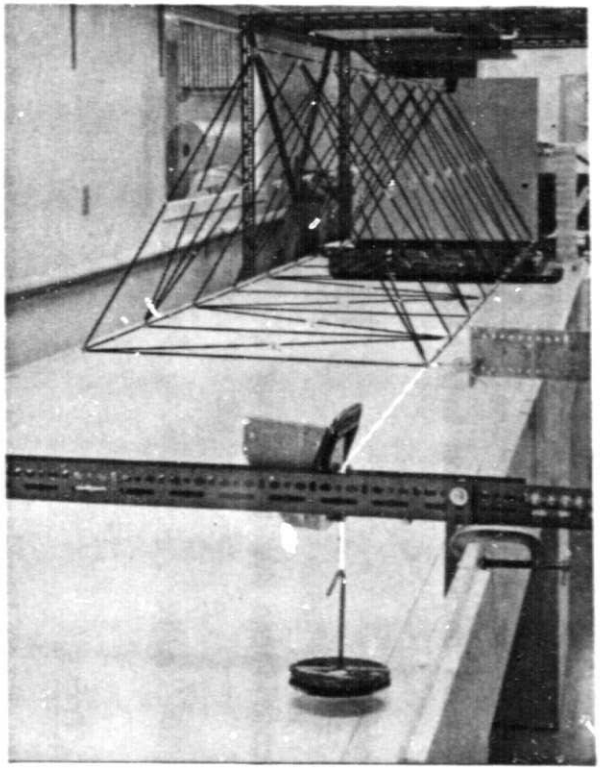

P087

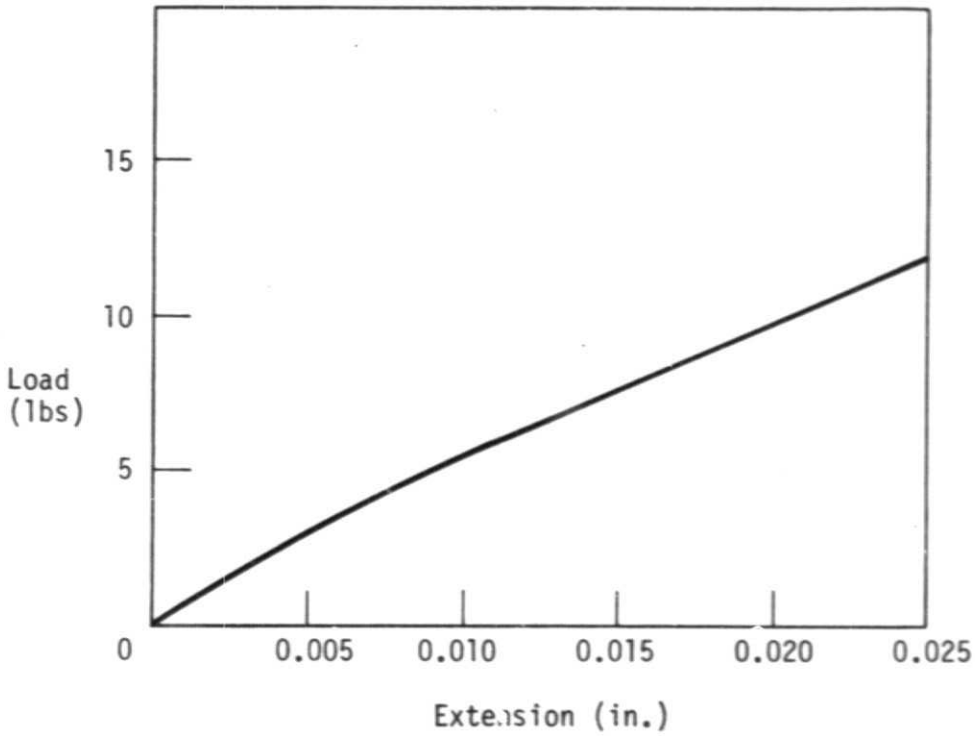

Figure 4-2. Longeron extension test.

196A

diagonals must be considered. A test was performed on a single diagonal to find the effect that the diagonal midhinge has on diagonal stiffness. Since it is not possible to measure the effect of the corner joints directly, the diagonal stiffness EA_d was determined from a lateral load test on a seven-bay beam.

4.2.2.1 DIAGONAL MIDHINGE

In order to find the effect that the diagonal midhinge has on diagonal stiffness, a diagonal was removed from the beam and tested in the same way as the longeron was tested in Section 4.2.1.1.

Axial loads of up to 35 N (8 pounds) in tension and up to 31 N (7 pounds) in compression were applied, and the results are shown in Figure 4-3. The diagonal stiffness is greater in tension than in compression, as is evident by the change in slope across the unloaded point - from 86,000 N/m in tension to 58,000 N/m in compression. The compliance of the midhinge, derived from averaging these data and deducting the compliance of the 0.83-m graphite/epoxy tube is

$$C_{d_m} = 1.30 \times 10^{-5} \text{ m/N}$$

4.2.2.2 TOTAL DIAGONAL

To find the total beam stiffness, the beam was cantilevered horizontally and loaded laterally at its tip through a structure which distributed the load such that torsion was not introduced. The test fixture was designed so that the load amount and direction are determined by the arrangement of hanging weights. Loads on the seven-bay test article were in the range -18 N (-4 pounds) $< F <$ +18 N (+4 pounds). Figure 4-4 shows the setup and results for this test. The slope of the curve indicates that the beam lateral stiffness is

$$\frac{F}{X} = 4500 \text{ N/m}$$

for this seven-bay beam (L = 3.0 m).

Equation (4-3), which gives total beam deflection due to bending and shear, yields diagonal stiffness

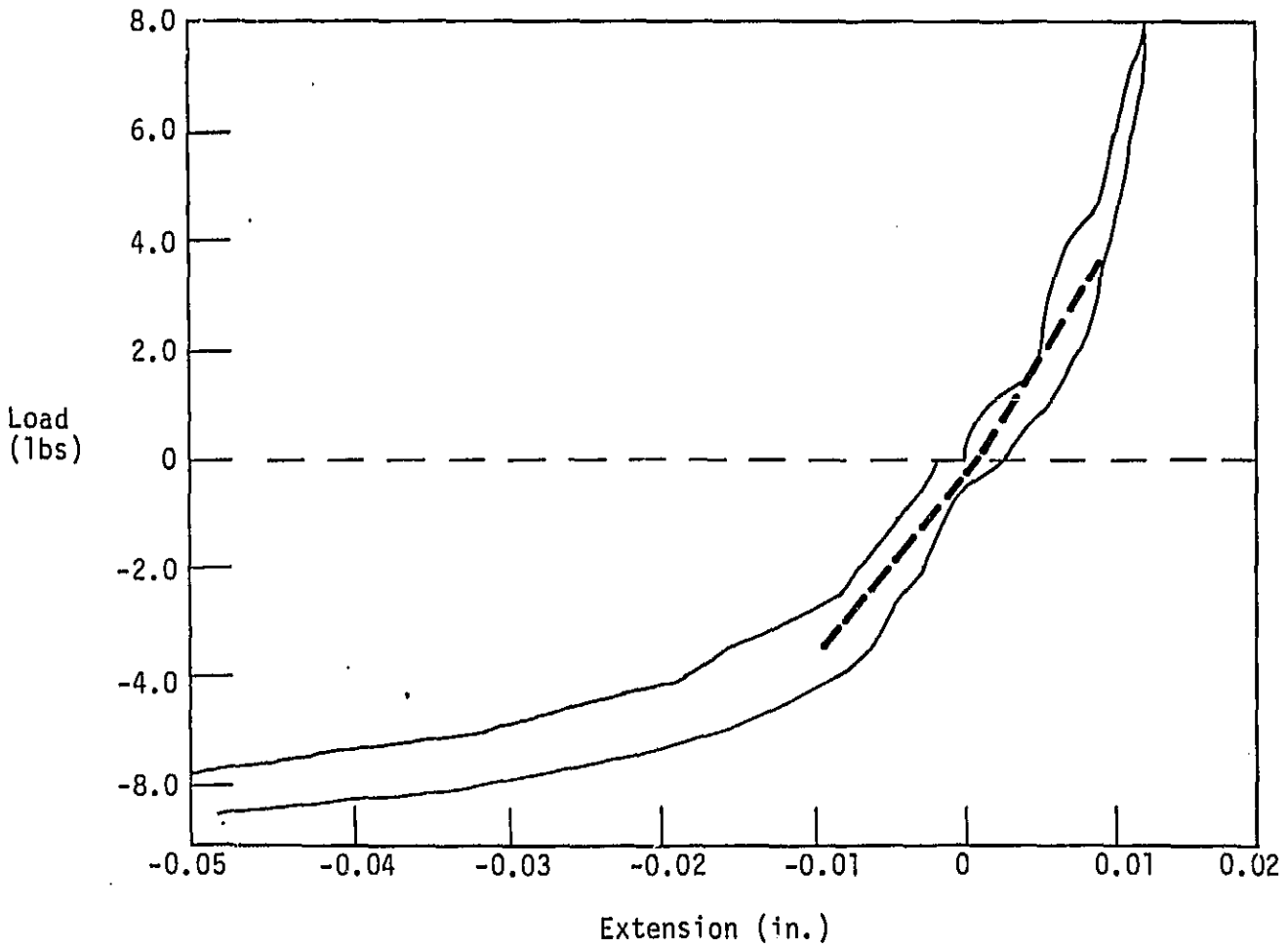

Figure 4-3. Individual diagonal stiffness test. 85-L009

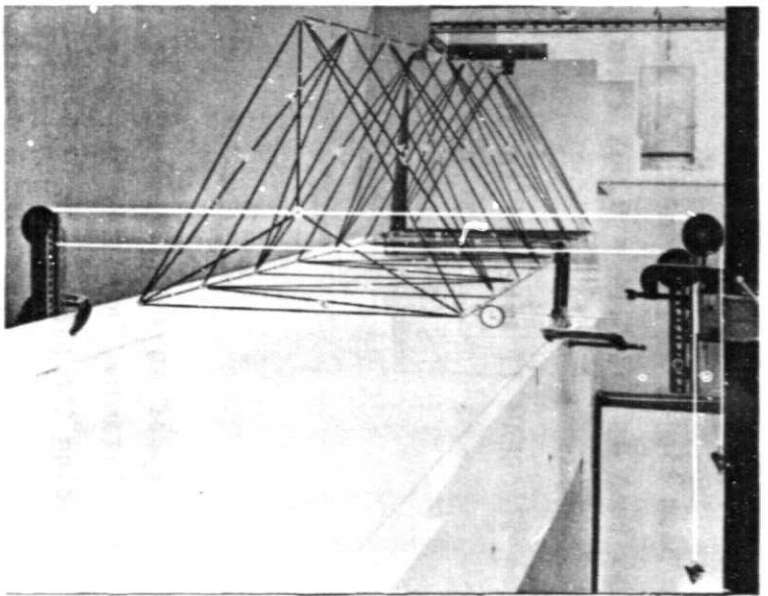

P088

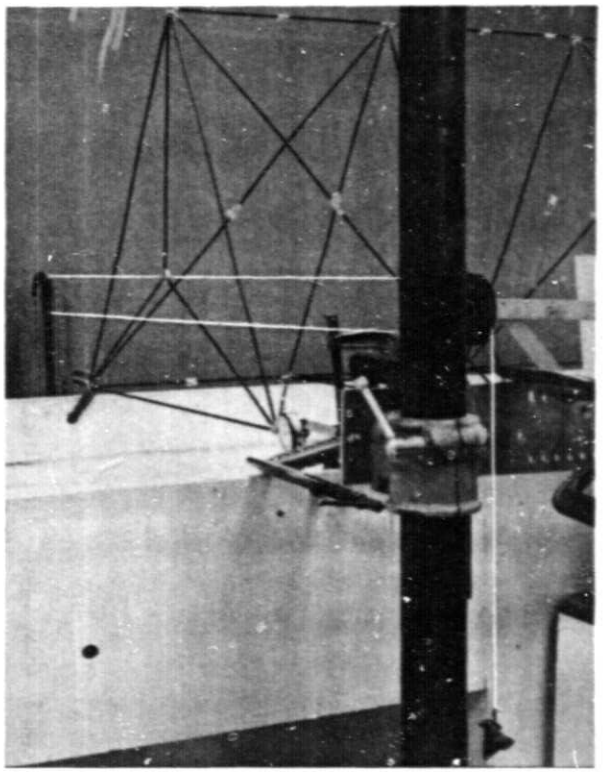

P089

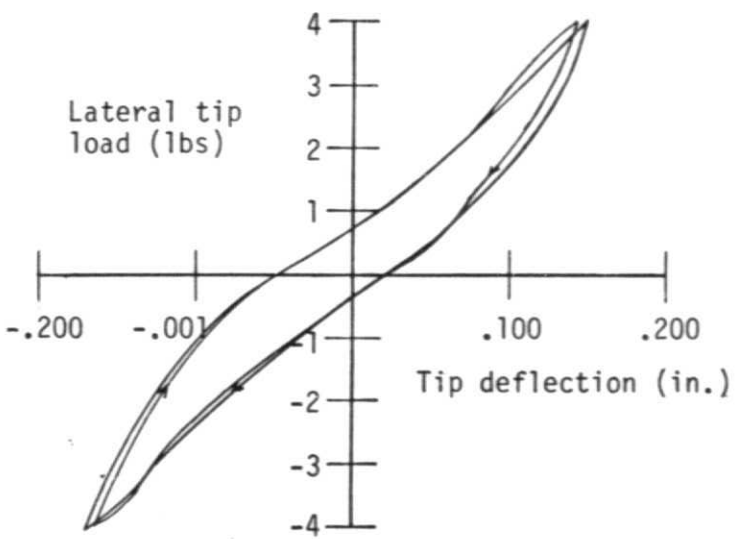

Figure 4-4. Beam lateral stiffness test.

197A

$$EA_d = \frac{2\, EA_\ell \frac{D^2}{L^2}}{\frac{9}{8} EA_\ell \frac{D^3}{L^3} \frac{X}{F} - 1}$$

$$= 43{,}000 \text{ N}$$

The diagonal compliance due to each of the ends was

$$C_{de} = 4.70 \times 10^{-6} \text{ m/N}$$

4.3 SYSTEM FREQUENCY

The experimental results obtained here allow for a determination of system frequency using the beam and deployer in their present status. The shear penalty, due to diagonal compliance in a beam of length L = 31.5 m is

$$k_s = 2 \frac{300{,}000}{43{,}000} \left(\frac{0.9}{31.5}\right)^2$$

$$= 0.0114$$

The beam deflection due to the load F at the beam tip is 1.0114 times that due to longeron strain alone. The beam stiffness then is 1/1.0114 = 0.989 times ideal beam stiffness.

The cantilever frequency of the existing STACBEAM II extended to 31.5 m and with a 54-kg blanket attached would be

$$f = \frac{\sqrt{3}}{\pi} \sqrt{\frac{(0.989)\, EI_{beam}}{M'L^4}}$$

The mass of the eight-bay STACBEAM II model is 1.032 kg and its length is 3.42 m. Replacement of the aluminum hinges with titanium increases the beam mass to 1.318 kg. The mass-per-unit length, including the blanket, is

$$M' = 1.318 \text{ kg}/3.42 \text{ m} + 54 \text{ kg}/31.5 \text{ m}$$

$$= 2.10 \text{ kg/m}$$

The beam stiffness is obtained using the results of Section 4.2.1.2.

$$EI_{beam} = \frac{3}{8} D^2 EA_{\ell}$$

$$= \frac{3}{8} (0.9 \text{ m})^2 (300{,}000 \text{ N})$$

$$= 91{,}000 \text{ Nm}^2$$

Then the cantilever frequency is

$$f = \frac{\sqrt{3}}{\pi} \sqrt{\frac{(0.989)(91{,}000)}{(2.10)(31.5)^4}}$$

$$= 0.12 \text{ Hz}$$

which is 60 percent of the design frequency of 0.2 Hz, but more than two times the measured frequency of the SAFE array, as discussed in the following section.

4.4 SYSTEM PERFORMANCE STATUS AND POTENTIAL

In the report for Phases I, II, and III of this project, a figure was presented which compared three beam candidates for support of a 53-kg solar blanket. The criteria for evaluation included system mass and cantilever frequency. The considered candidates were the Astromast, Extendible Support Structure (ESS), and the STACBEAM. The portion of the figure relating to STACBEAM is shown in Figure 4-5 which compares STACBEAM performance status and potential with that of the SAFE array as flown and normalized for blanket mass.

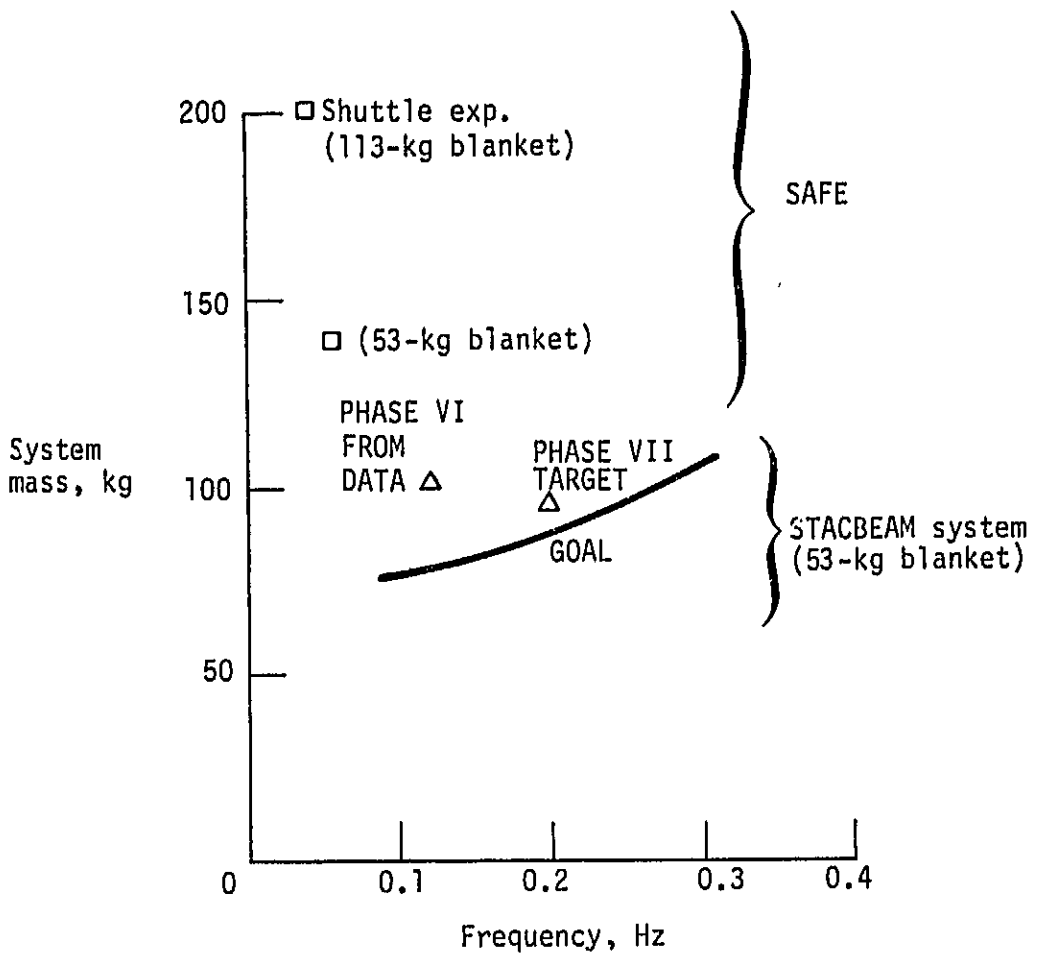

Figure 4-5. System performance.

85-L005

It is now possible to evaluate the STACBEAM system in terms of the engineering models already constructed. In Reference 2 (p. 40), the masses of the various components in the system are tabulated for a point design in which the system frequency is 0.2 Hz. In particular, the system mass using a STACBEAM as a mast was estimated to be 89.8 kg, where the beam mass is listed as 10.0 kg and the deployer mass is listed as 6.4 kg. According to the data given in the previous section, the mass of the 31.5-m beam can now be estimated at 12.2 kg, where the increase is due to greater than predicted hinge mass. The deployer, as designed and constructed during Phase V (Ref. 3, p. 22) has a mass of 15.5 kg. The system mass is newly estimated at 101.1 kg. The frequency, as predicted in the previous section, would be 0.12 Hz. This point (0.12 Hz, 101.1 kg) is shown in Figure 4-5.

The potential for moving this point to the right and down (higher frequency, lower mass) is seen as follows. System frequency depends not only on beam stiffness but also on beam mass. The former can be further increased over STACBEAM II primarily by improving the hinge pin designs so that their compliance is minimized. In STACBEAM II, the hinge pins are threaded on one end for retention and are larger than those in STACBEAM I to decrease compliance. It has been shown that these objectives of better retention and lower compliance can be met more efficiently by using hinge pins which are press-fit into one part and close-fit in the other (Ref. 5). Other efforts toward increasing beam stiffness include the use of titanium hinges in the engineering model and doubling the longeron cross-sectional area. The latter would be done by using rods which are slightly smaller than the tubular outer diameter but twice the area. The increased longeron mass would be compensated for by reducing the batten and diagonal areas. These efforts are expected to increase the system frequency to 0.20 Hz.

Beam mass cannot be decreased appreciably. Although use of higher modulus fibers would require less graphite mass and some effort on hinge design could decrease their mass, the added complexity incurred due to the inclusion of continuous deployment capability (Section 5) will increase the corner body masses. The deployer mass, however, can be decreased through the

use of composite materials. These were not included in the deployer engineering model of Phase V for cost reasons and would reduce its mass by 5 kg so that the system mass is 96 kg. This point (0.20 Hz, 96 kg) is shown in Figure 4-5 as a target for Phase VII.

Also shown in Figure 4-5 is the mass and frequency of the SAFE experiment which was conducted on the Shuttle flight of July 1984. System mass was 200 kg, of which 113 kg was the blanket. The system frequency was 0.037 Hz. This point is not a valid comparison, however, because the SAFE blanket mass was higher than that of the system used in this design analysis. Theoretical reduction of the SAFE system mass by 60 kg and increasing the frequency by the factor $\sqrt{113/53}$ results in a frequency of 0.054 Hz and a system mass of 140 kg. This theoretical point represents a SAFE data point that is mass-adjusted for a 53-kg blanket.

The STACBEAM/solar array system status can then be compared to the mass-adjusted SAFE array as follows:

- The STACBEAM system frequency is 2.2 times that of the mass-adjusted SAFE array
- The STACBEAM system mass is 39 kg less than that of the mass-adjusted SAFE array

The potential of the STACBEAM/solar array system, realized primarily by improving longeron stiffness, predicts a system frequency of 3.7 times the mass-adjusted SAFE array with a mass savings of 44 kg.

SECTION 5
RETRACTION AND CONTINUOUS DEPLOYMENT CONCEPTS

The deployer developed in Phase V of this contract is of the reciprocating type, in that it erects one bay of the STACBEAM in a sequence of operations which must be repeated, after some dead time, for erection of the next bay. Approximately 14 seconds are required per bay for an average deployment speed of 0.03 m/s. There is no provision for retraction.

The basic requirement for retraction for continuous or reciprocating action is a highly synchronized mechanism which initiates folding of the longerons and diagonals. An implied need is that the stack be lifted so that a bay cannot redeploy after it has been retracted. Lastly, because the stack must be lifted, the attached solar blanket package must also be lifted at the same rate as the stack. A method of lifting the stack at a metered rate is discussed for the case of continuous deployment later in this section.

Continuous deployment is preferred over reciprocating deployment for four reasons:

1. Time - It takes less time for continuous deployment or retraction because there is no dead time between the deployment of each successive bay as with the reciprocating method where the mechanism has to reset between each bay deployment.
2. Dynamics - The continuous system is less complex dynamically in that the elements move at a constant velocity during deployment or retraction whereas the elements making up the reciprocating system are constantly accelerating with stops and starts for each bay that is deployed.
3. Complexity - For the continuous system, the motions of the separate elements are related through gearing. With the reciprocating system on the other hand, the separate elements (such as the jaws and lead screws) must have separate electronic controls to synchronize their actions.
4. Weight - The open tube of the reciprocating deployer will be replaced by a closed tube for the continuous deployer which will require less bracing and will therefore be lighter.

The method of continuous deployment discussed here uses lead screws which interface directly with the beam corner hinges. Another method is possible using recirculating graspers on a chain (or belt) drive.

5.1 CONTINUOUS DEPLOYMENT

The method of continuous deployment is shown in Figures 5-1 through 5-6. The deployer itself is deployable, as was the deployer of Phase V, so that the launch height is slightly more than the baylength or the stack height, whichever is greater. Lead screws which lift the beam in a sequential manner are threaded through the corner fittings at launch. The first operation after launch is the rotation of the lead screws out of the stack so that only the top batten frame remains threaded. An independent drive system will raise the lead screws to synchronize with their rotation. When the deployer is fully deployed, the lead screws stop and the deployer is locked in this configuration so that the lead screws remain at this height throughout deployment.

Rotation of the lead screws in the opposite direction then lifts the top batten frame and erects the first bay. The next batten frame is held by synchronized latches so that it is released to engage the lead screws only if sufficient turns of the lead screw have occurred. Each corner body engages the lead screw thread at the correct location since it is connected to another corner body on the lead screw through a fully extended longeron. Thus, full deployment of each bay is assured while constant lead screw rotation rate deploys the beam at constant velocity.

Rotation of the lead screws continues until full beam deployment or until a partial deployment position is reached. Beam root rigidity is maintained through rigidity of the lead screws which are held in the deployer as described below.

5.1.1 Lead Screw Design

The main features of each lead screw and its support are shown in Figure 5-4. Starting at the lower end (toward the stack), the significant features are:

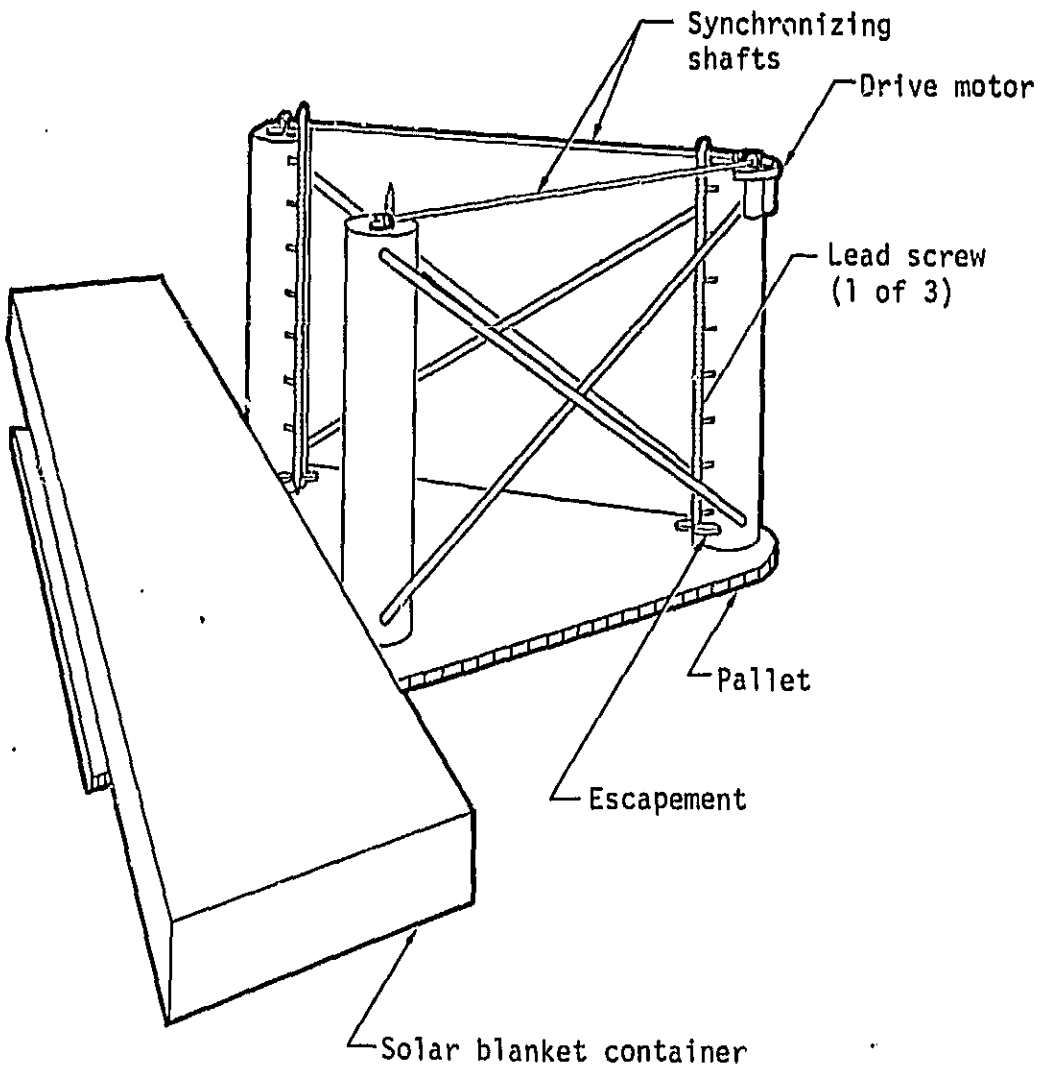

Figure 5-1. Deployer, launch configuration. 204A

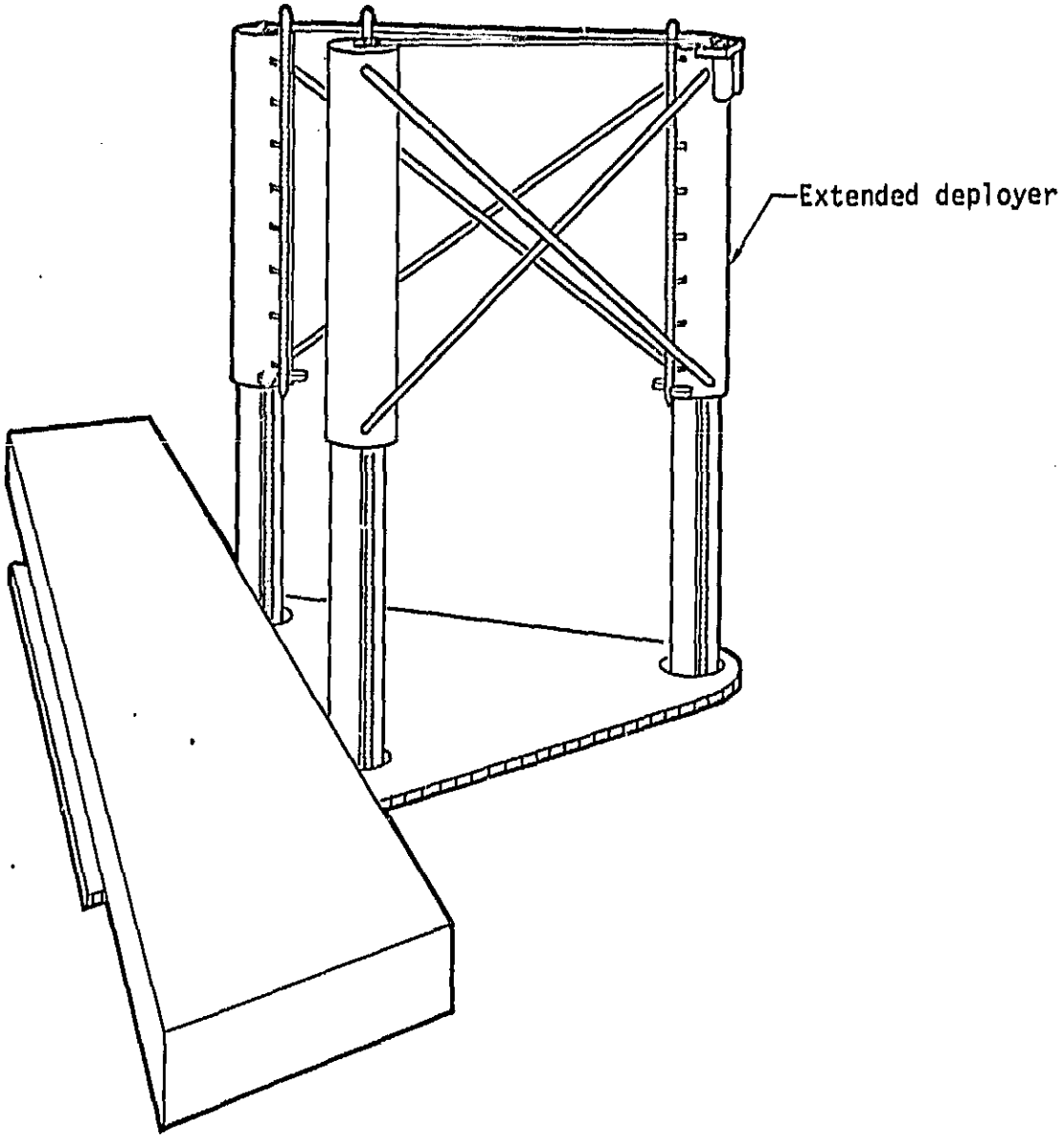

Figure 5-2. Deployer, extended. 205A

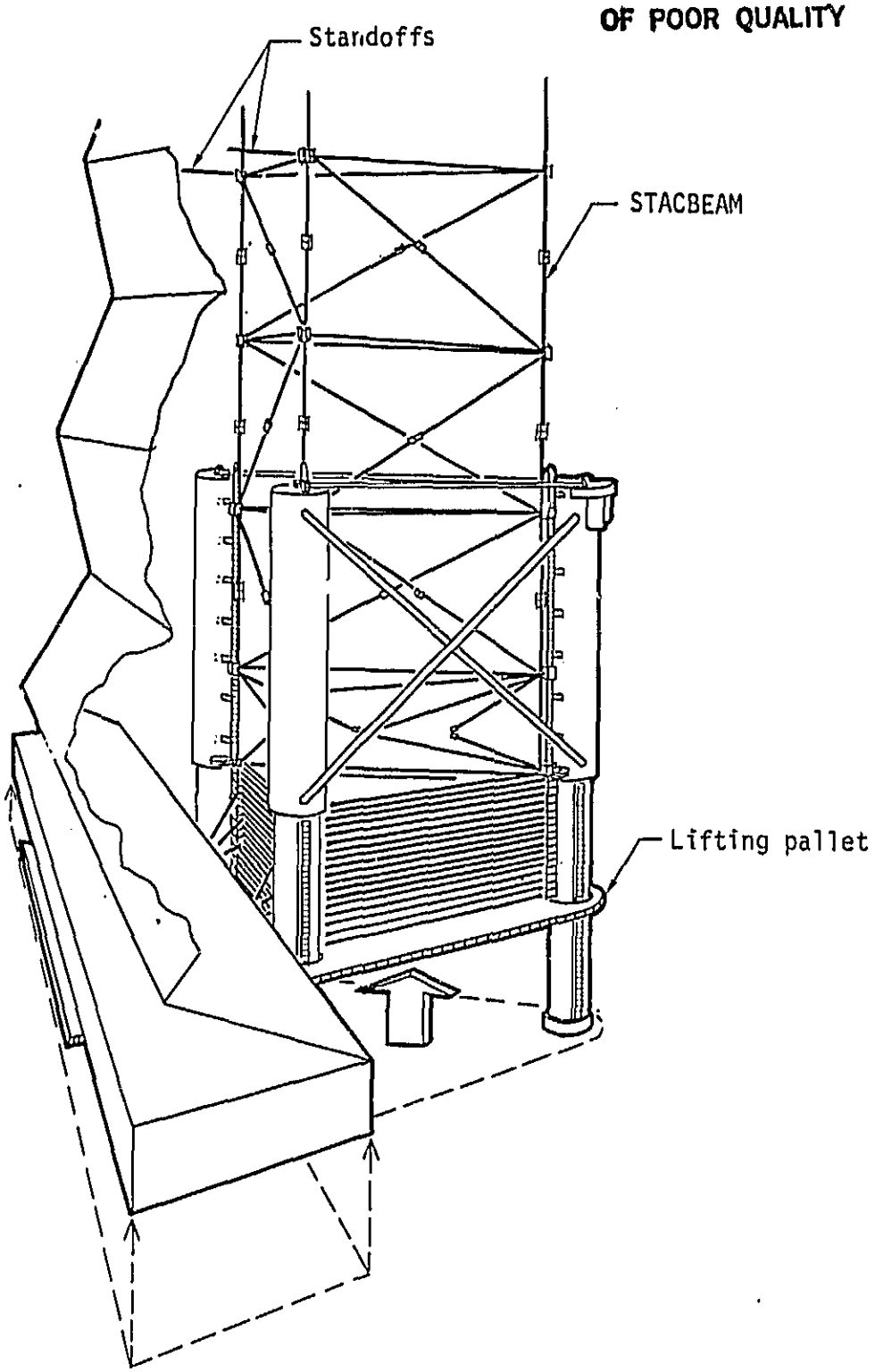

Figure 5-3. Deployer in operation. 206A

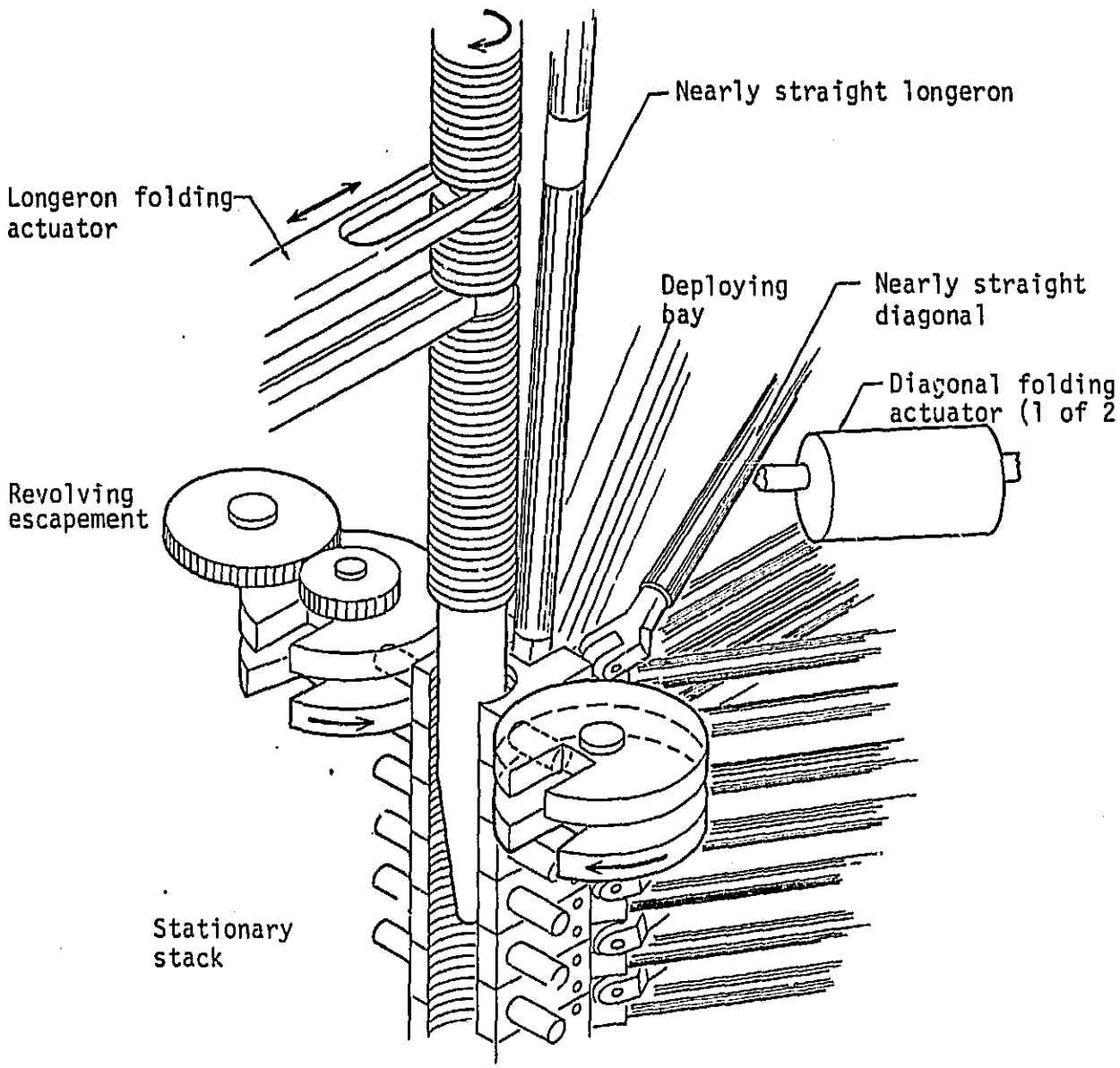

Figure 5-4. Deployer detail with deploying bay. 207A

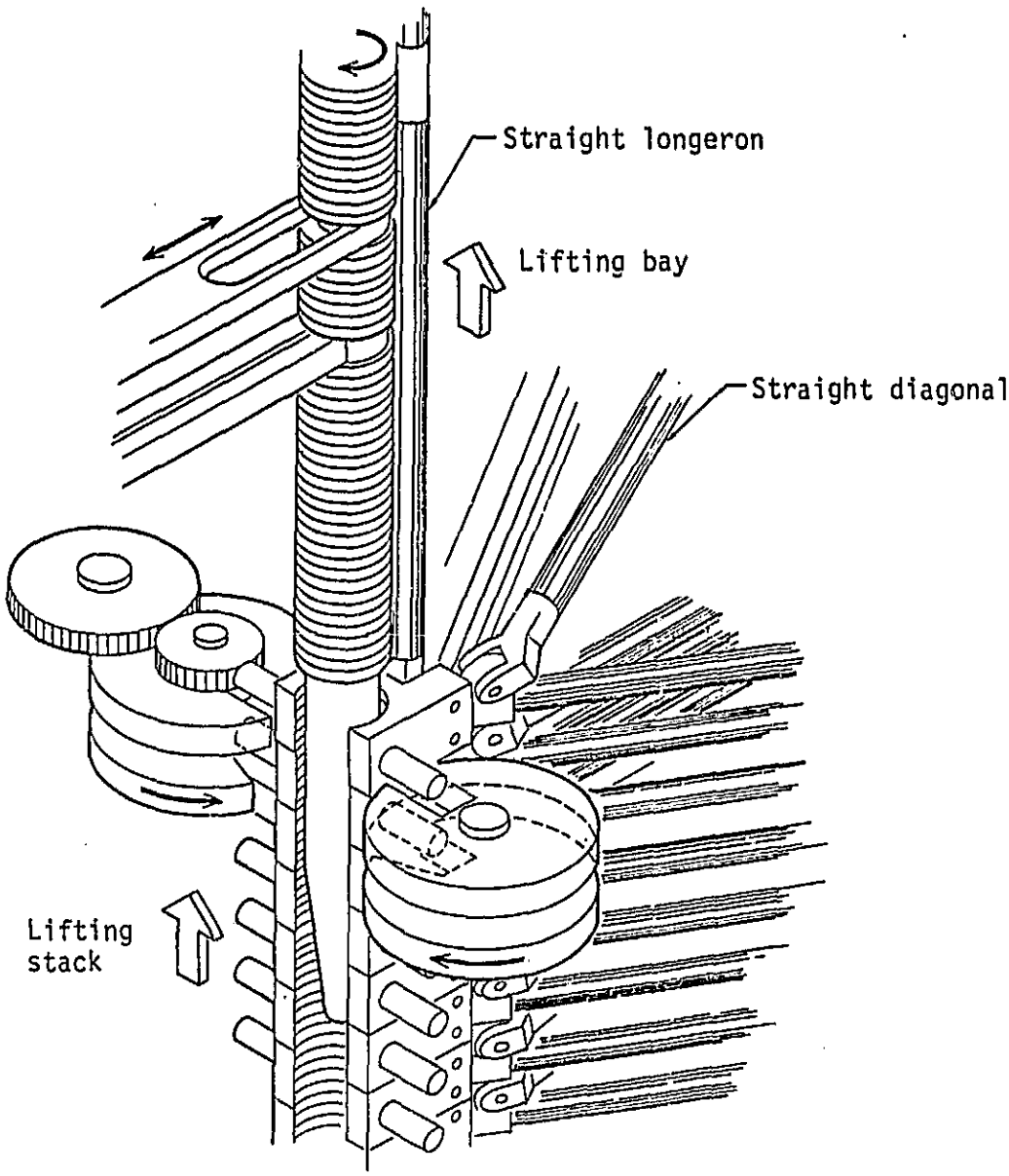

Figure 5-5. Deployer detail with lifting stack and bay. 207A-1

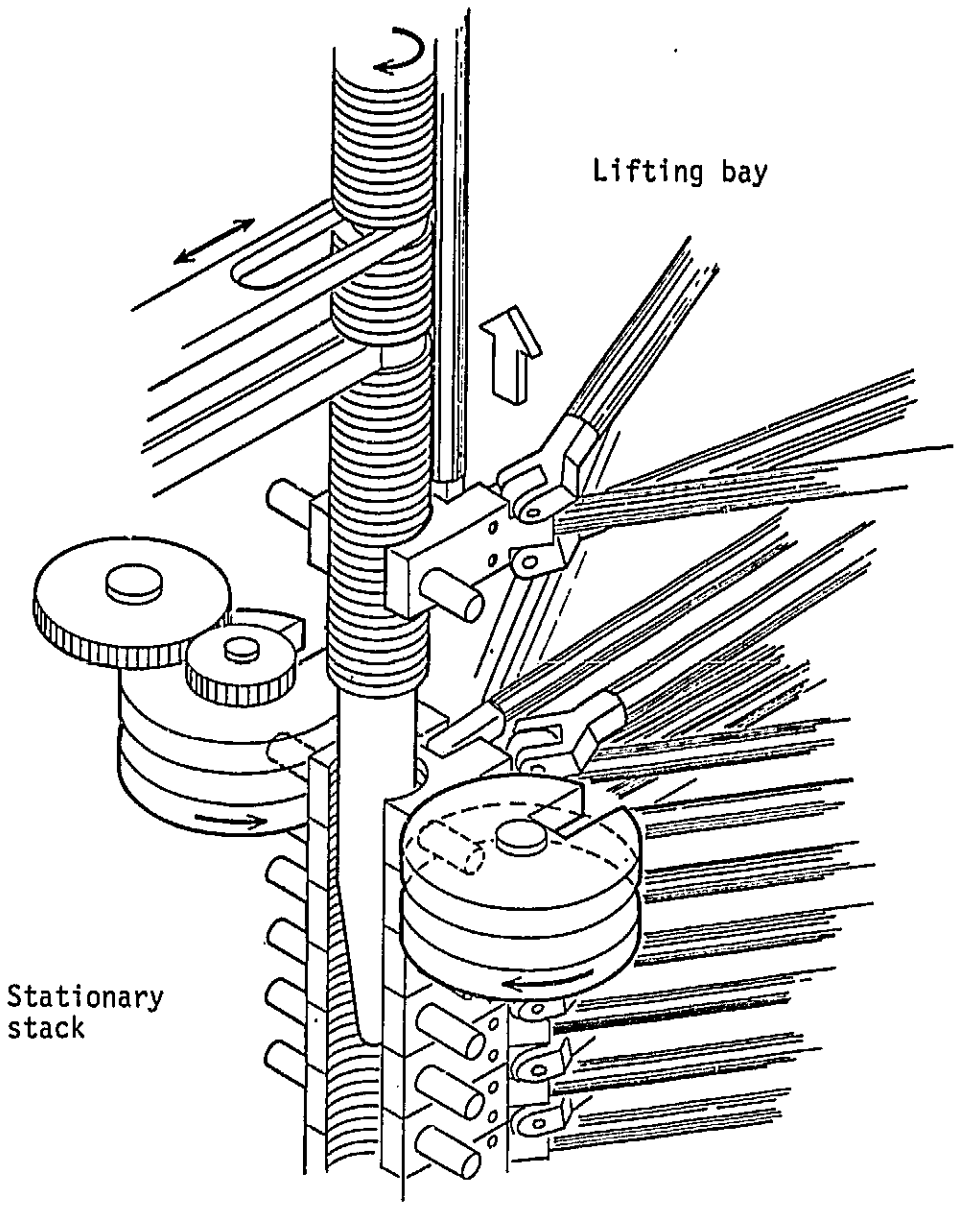

Figure 5-6. Deployer detail with lifting bay and stationary stack.

207A-2

- o Tapered end to guide open-nut fittings onto lead screw
- o Untapered, unthreaded section to orient fitting
- o Threaded portion
- o Widened thread gap near lower end to allow for differential thermal expansion
- o Several lateral supports
- o Teeth for gear drive
- o Untapered, unthreaded section near top
- o Tapered top end to aid in retraction

It was noted earlier that during deployment the stack must be lifted. The mechanism shown in Figures 5-4 to 5-6 causes this to happen in discrete increments such that the stack base is lifted a distance equal to the packaged batten spacing immediately after each bay comes to full extension. The key element in the mechanism is the revolving gate which allows one corner hinge to exit and another to enter each time the lead screw has rotated sufficiently to lift the beam one bay length. Since the stack is actively lifted, the batten frame held by the revolving gate is at once the top of the stack as well as the base of the deploying bay.

This approach works equally well in the retraction and deployment modes. No assist is needed in straightening members during deployment since the midhinges provide alignment forces. During retraction, active folding of the longerons and diagonals must occur at specific times which are determined by beam position relative to the deployer.

5.2 RETRACTION

Folding of the longerons and diagonals during retraction is accomplished by the mechanisms shown in Figure 5-4. Passage of the corner hinge down the lead screw actuates the mechanisms which simultaneously push on the longeron and diagonal members. Actuation would be by motion-enhancing levers operating directly off beam motion, or by electrical position sensing. Advantages of the former system include inherent synchronicity, since the levers necessarily track beam position, and relative simplicity compared to an electrically actuated system.

Near the base of the lead screws, the thread gaps widen at constant pitch, as discussed in Section 5.1.1, to allow for differential thermal expansion. During retraction, this extra room can be used for premature folding to ensure that each bay has started folding before its base batten frame actually enters the escapement.

5.3 SOLAR BLANKET DEPLOYMENT

The solar blanket will be attached to the beam by pairs of standoffs located every eight bays. The standoffs will be made from the same graphite/epoxy tubing as is used in the beam and will be hinged at their points of attachment to the beam, except at the top of the beam where the blanket will be rigidly supported.

When the beam is in its retracted position, the blanket will be tightly folded and the top of the blanket will be level with the top of the beam. The standoffs are consecutively longer towards the bottom of the beam. As the beam is deployed and the blanket unfolds, each standoff first pushes the edge of the blanket up until the standoff is normal to the beam and the blanket above the standoff is taut. The blanket continues to unfold until the next standoff begins to move out of the deployer. After the mast is fully deployed, the last section of the blanket is pulled taut by a spring. During retraction, the steps are reversed.

SECTION 6
CONCLUSIONS AND RECOMMENDATIONS

The STACBEAM was conceived in an early phase of this contract as a deployable structure for support of a solar array blanket. In tradeoff studies, it compares favorably with the Astromast and Extendible Support Structure in terms of total system mass, package volume, frequency, and complexity. Structural advantages, all of which increase system frequency, include:

- o Increased beam depth without significant increase in deployer mass
- o Blanket partitioning by deployable standoffs
- o Single-degree-of-freedom hinges which allow the use of material of high modulus and cross section

The fabrication and test of STACBEAMs I and II indicate a reduction of beam stiffness, due to hinge compliance, so that the measured beam stiffness is less than the targeted goal. Comparison to the recently conducted SAFE experiment, however, indicates that the STACBEAM in its present status will support an array at more than twice the frequency than that attainable with currently flying deployable structures, at a decreased total system mass. Efforts toward decreasing hinge compliance promise even greater advantages gained with use of STACBEAM technology.

It is apparent that a continuous deployment system has several advantages over a reciprocating system. These advantages are a shorter deployment time, dynamic stability, less complexity, and a lower weight. A continuous deployer should be designed and built and there should be several ground tests with and without the solar blanket attached to assure smooth operation.

It is recommended that a demonstration system be designed and fabricated, including a continously operating deployer with retraction capability which interfaces with a compatible STACBEAM and a mockup of a solar blanket which is attached to the STACBEAM by standoffs. Design efforts will be directed toward attaining the targeted system frequency goal of 0.2 Hz by reducing longeron compliance and system mass.

APPENDIX A
NEARLY-OVER-CENTER HINGE ANALYSIS

APPENDIX A
NEARLY-OVER-CENTER HINGE ANALYSIS

A hinge has been developed at Astro which allows a pair of linear members to rotate a full 180 degrees relative to each other which provides a preload in the aligned configuration. This preload acts to hold the member centerlines colinear and provides forces which drive a deploying structure toward full deployment.

Figure A-1 shows various views of a recently fabricated design. In this particular use, the hinge does not rotate a full 180 degrees, and the hinge pin is not orthogonal to the member centerline. These features were necessary because of the structural configuration and do not affect the analysis here.

Consider four hinge pins (a, b, c, and d) which are shown in Figure A-1. The pins connect four members as follows:

- o ab is a link
- o ac is a link
- o bd is part of the right rotating member
- o cd is part of the left rotating member.

Figure A-2 shows these members schematically. The hinge pins are assumed to rotate freely in their holes, and moments are generated due to torsion springs. The following analysis is for the general case in which torsional springs act as Pins a and c. No consideration is made for springs at Pins b and d because of the half-turn of unwinding between the packaged and deployed configuration.

It is shown in Figure A-2 that the vertical loads V are all of the same magnitude; the signs vary according to equilibrium requirements. The horizontal loads F are similarly equal. The vertical load is determined by summing moments at c

$$\sum M_c = -M_c + M_a - V\ell_{ac} = 0$$

Then,

$$V = \frac{M_a - M_c}{\ell_{ac}}$$

ORIGINAL PAGE IS
OF POOR QUALITY

Figure A-1. Kinematics of nearly-over-center hinge.

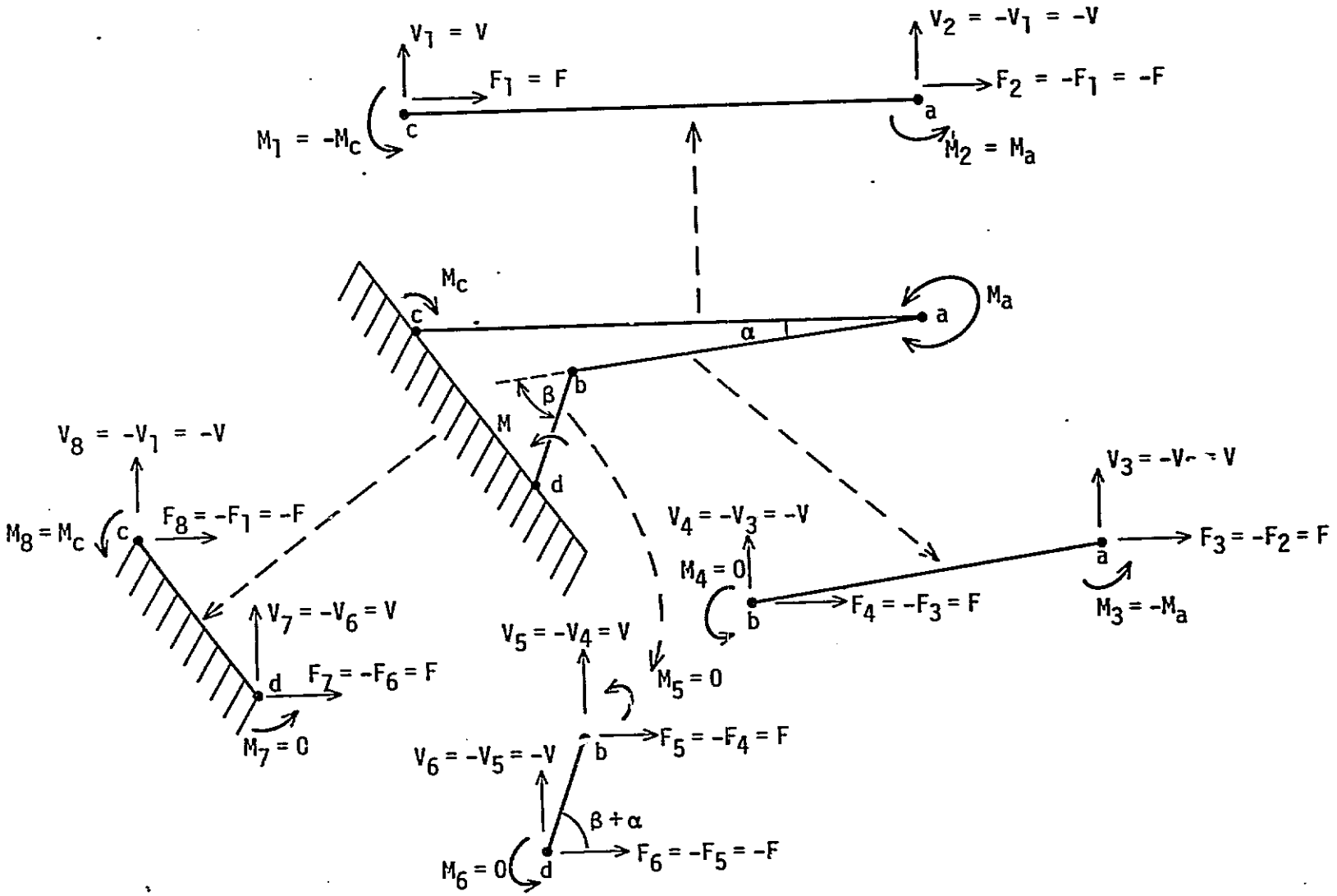

Figure A-2. Equilibrium forces and moments in nearly-over-center hinge.

The horizontal load is determined at Point b.

$$\sum M_b = -M_a + V\ell_{ab} \cos \alpha - F\ell_{ab} \sin \alpha = 0$$

Then

$$F = \frac{M_a - M_c}{\ell_{ac} \tan \alpha} - \frac{M_a}{\ell_{ab} \sin \alpha}$$

The moment generated in the right rotating member (bd) which must be overcome in order to open the hinge is

$$M = -F\ell_{bd} \sin (\alpha + \beta) + V\ell_{bd} \cos (\alpha + \beta)$$

$$= \left(\frac{M_c - M_a}{\ell_{ac} \tan \alpha} + \frac{M_a}{\ell_{ab} \sin \alpha} \right) \ell_{bd} \sin (\alpha + \beta) + \frac{M_a - M_c}{\ell_{ac}} \ell_{bd} \cos (\alpha + \beta)$$

Rearranging yields

$$M = \frac{\ell_{bd}}{\ell_{ac}} \frac{\sin \beta}{\sin \alpha} \left\{ M_c + M_a \left[\frac{\ell_{ac}}{\ell_{ab}} \left(\frac{\sin \alpha}{\tan \beta} + \cos \alpha \right) - 1 \right] \right\}$$

It is seen that for small α and for $\ell_{ac}/\ell_{ab} \simeq 1.2$ the second term above is relatively small so that the effectiveness of the spring at Point a is small. Making $M_a = 0$ in the above equation (deleting spring a) results in

$$\frac{M}{M_c} = \frac{\ell_{bd}}{\ell_{ac}} \frac{\sin \beta}{\sin \alpha} \qquad (1)$$

Alternately, the moment factor can be obtained for the simple case in which only Pin c has a spring by noting that Link ab is loaded by pure compression P (no moment or shear). Then balancing moments at Point c yields

$$-M_c + \ell_{ac} P \sin \alpha = 0$$

At Point b, the moment generated in the right hinge member due to compressive load P acting on Point b is

$$M = \ell_{bd} P \sin \beta$$

Cancelling the load P then yields the moment factor above.

EXAMPLE - TRUSS BEAM MODEL DESIGN

The hinge of Figure 1 was designed and fabricated as follows:

ℓ_{bd} = 0.375 inch
ℓ_{ac} = 2.455 inch
α = 5.37 degrees
β = 65.07 degrees

One torsion spring is used at Pin c. The moment factor obtained is

$$\frac{M}{M_c} = 1.48$$

The measured opening moment for this device was M = 30 in-lb, arising from a spring moment of M_c = 20 in-lb.

PRELOAD

The configuration of this hinge was special in two respects: 1) Pins b and c are on the deployed member centerline, and 2) Pins b and d form a line perpendicular to the centerline. Then the preload along the centerline is

$$P_r = \frac{M}{\ell_{bd}} = 80 \text{ pounds}$$

which is the tensile load in the deployed member which just causes the hinge to open.

A measure of the compliance contributed by the nearly-over-center hinge in tension can be obtained as follows. The 80-pound tensile load which opens the hinge will cause three hinge pins to approach colinearity. These are the extreme end pins in the member, which in this case are on the centerline, and separated about 60 inches from each other, and Pin d in the hinge which is 0.375 inch off the centerline. The member length increase is 0.0047 inch when the three hinges are colinear. The compliance is

$$\frac{0.0047 \text{ in.}}{80 \text{ lbs}} = 6 \times 10^{-5} \text{ in/lb}$$

$$= 3.3 \times 10^{-7} \text{ m/N}$$

after the preload is overcome. The compliance under compression loads should be much smaller since it will be due only to deformations at the two preloaded mating surfaces.

Stability

The closing moment which drives the unfolding member toward full deployment varies according to the values of the angles α and β which change as the members rotate (as Pin b rotates about Pin d). A computer program was developed which calculates these angles according to the rotated position θ and determines the moment factor M/M_c as it changes during deployment. Figure A-3 shows the results which are described as follows. At $\theta = 0$, the mechanism is at full deployment and M/M_c is maximum at 30 in-lb. For $\theta < 38$ degrees, M/M_c is greater than zero and drives toward deployment. For $\theta > 38$ degrees, a relatively low force is required to extend the member.

Conclusions

Examination of Equation (1) and its derivation yields the following conclusions:

- Of the four possible spring positions (at the four pin locations), only one is efficient in terms of generating high bending moment. Two of the positions are inefficient due to spring unwinding during deployment; one simply does not produce moment multiplications. Position c is preferred because it produces high moment multiplication and does not unwind during deployment.
- The angle between the pins must be very small in the fully deployed position.
- The unsprung link must be properly oriented so that its compressive load not only preloads the joint but also produces the desired moment between the hinged members.

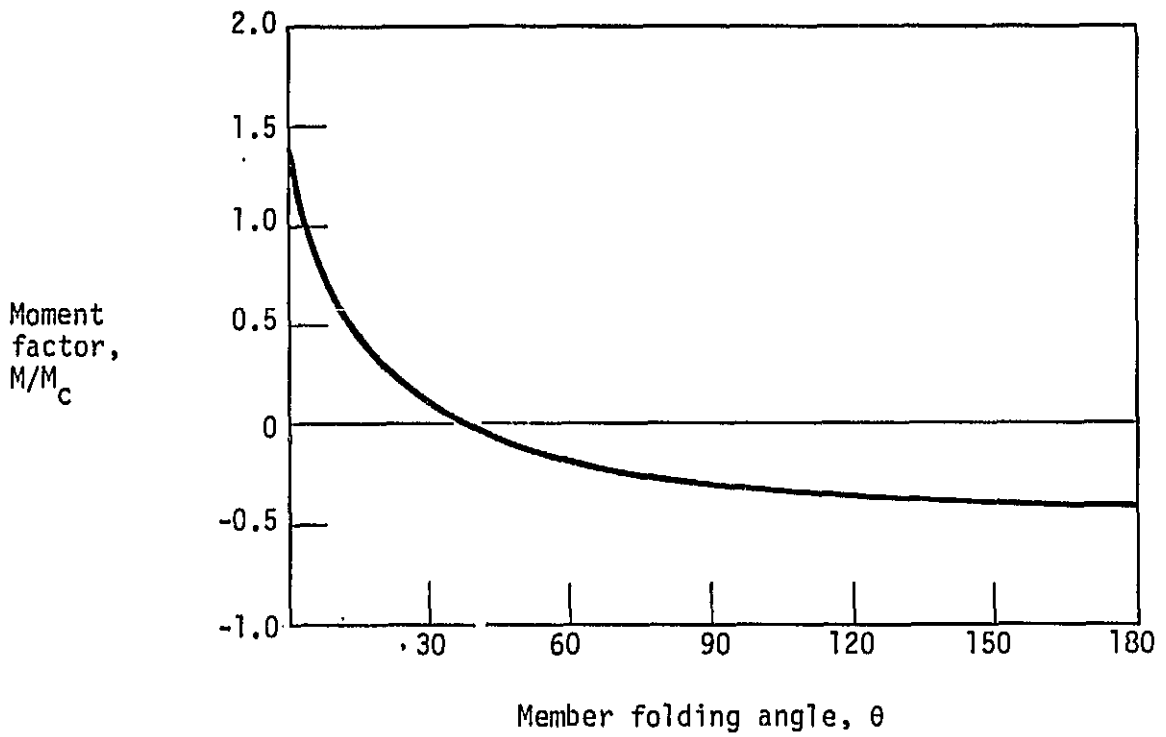

Figure A-3. Effect of member folded angle on moment factor.

APPENDIX B
BEAM DEFLECTION ANALYSIS

APPENDIX B
BEAM DEFLECTION ANALYSIS

The following is an analysis to determine the equations governing beam deflection arising from diagonal strain. The loads in the diagonal are determined for the case of a radially directed load passing through a corner body.

Resulting values are used to find the strain in the diagonals and finally to determine the relationship between the diagonal stiffness and the beam deflection.

We assume that the strain in the longeron does not affect the deflection due to diagonal strain because the diagonal and longeron strains are linearly additive.

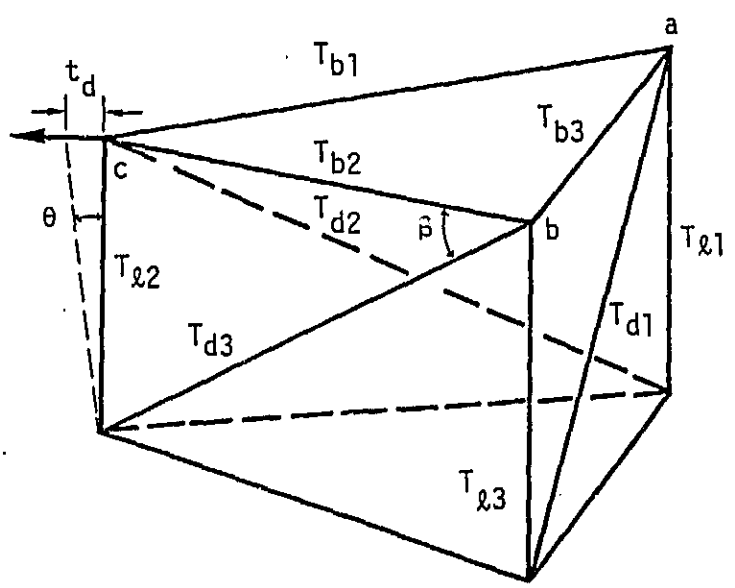

The force equations are as follows. At Point a,

$$x) = -T_{b1} \cos 30 = 0$$

$$y) = -T_{b1} \sin 30 - T_{b3} - T_{d1} \cos \beta = 0$$

$$z) = -T_{d1} \sin \beta - T_{\ell 1} = 0$$

At Point b,

$$x) = -T_{b2} \cos 30 - T_{d3} \cos \beta \cos 30 = 0$$

$$y) = T_{b2} \sin 30 + T_{d3} \cos \beta \sin 30 + T_{b3} = 0$$

$$z) = -T_{d3} \sin \beta - T_{\ell 3} = 0$$

At Point c,

$$x) = (T_{b1} + T_{b2} + T_{d2} \cos \beta) \cos 30 - F = 0$$

$$y) = (T_{b1} - T_{b2} + T_{d2} \cos \beta) \sin 30 = 0$$

$$z) = -T_{d2} \sin \beta - T_{\ell 2} = 0$$

Solving the above equations simultaneously gives the following results:

$$T_{b1} = 0 \qquad T_{b2} = \frac{F}{2 \cos 30} \qquad T_{b3} = 0$$

$$T_{\ell 1} = 0 \qquad T_{\ell 2} = \frac{F \tan \beta}{2 \cos 30} \qquad T_{\ell 3} = \frac{F \tan \beta}{2 \cos 30}$$

$$T_{d1} = 0 \qquad T_{d2} = \frac{F}{2 \cos \beta \cos 30} \qquad T_{d3} = \frac{-F}{2 \cos \beta \cos 30}$$

The strain in the diagonals is

$$\theta = \frac{\delta d/\ell}{\cos \beta \cos 30} = \frac{2F}{3 \cos^2 \beta \, EA_d \, \ell/d}$$

Since $\ell/d = \sin \beta$, the lateral deflection X_d is

$$X_d = \theta L = \frac{2\,FL}{3 \cos^2 \beta \sin \beta\, EA_d}$$

In the STACBEAM, $\beta = 30$ degrees. Then beam deflection due to diagonal strain is

$$\frac{X_d}{F} = \frac{16}{9} \frac{L}{EA_d} \qquad \text{(B-1)}$$

It can be shown that this relation holds in any loading direction.

Beam deflection due to longeron strain is given by

$$X_\ell = \frac{FL^3}{3\,EI}$$

where I is the moment of inertia of the beam section. For three longerons in a triangular configuration,

$$\begin{aligned} I &= \Sigma\, x^2 A \\ &= r^2 A_\ell + \left(\frac{r}{2}\right)^2 A_\ell + \left(\frac{r}{2}\right)^2 A_\ell \\ &= \frac{3}{2} r^2 A_\ell \\ &= \frac{3}{8} D^2 A_\ell \end{aligned}$$

Then beam deflection due to longeron strain is

$$\frac{X_\ell}{F} = \frac{8}{9} \frac{L^3}{D^2\, EA_\ell} \qquad \text{(B-2)}$$

REFERENCES

1. Scott-Monck, John; and Stella, Paul M.: Recent Developments in High Performance Planar Solar Array Technology. Proceedings of the 19th IECEC, 1984, Volume 1, p. 78.

2. Adams, Louis R.; and Hedgepeth, John M.: Efficient Structures for Geosynchronous Spacecraft Solar Arrays, Phase I, II, and III Final Report. Astro Research Corporation, ARC-TN-1098, 14 September 1981.

3. Adams, Louis R.: Efficient Structures for Geosynchronous Spacecraft Solar Arrays, Phase IV. Astro Research Corporation, ARC-TN-1112, 14 September 1982.

4. Adams, Louis R.: Efficient Structures for Geosynchronous Spacecraft Solar Arrays, Phase V Final Report. Astro Research Corporation, ARC-TN-1125, 27 September 1983.

5. Adams, Louis R.; and Hedgepeth, John M.: BAT BEAM. ARC-TN-1130, Astro Aerospace (Research) Corporation, 16 July 1984.